© 2015. Published by The Company of Biologists Ltd | Development (2015) 142, 983-993 doi:10.1242/dev.113449

RESEARCH ARTICLE

Muscle composition is regulated by a Lox-TGFβ feedback loop

Liora Kutchuk[1,*], Anu Laitala[2,*], Sharon Soueid-Bomgarten[1], Pessia Shentzer[1], Ann-Helen Rosendahl[2], Shelly Eilot[1], Moran Grossman[3], Irit Sagi[3], Raija Sormunen[4], Johanna Myllyharju[2], Joni M. Mäki[2] and Peleg Hasson[1,‡]

ABSTRACT

Muscle is an integrated tissue composed of distinct cell types and extracellular matrix. While much emphasis has been placed on the factors required for the specification of the cells that comprise muscle, little is known about the crosstalk between them that enables the development of a patterned and functional tissue. We find in mice that deletion of lysyl oxidase (Lox), an extracellular enzyme regulating collagen maturation and organization, uncouples the balance between the amount of myofibers and that of muscle connective tissue (MCT). We show that Lox secreted from the myofibers attenuates TGFβ signaling, an inhibitor of myofiber differentiation and promoter of MCT development. We further demonstrate that a TGFβ-Lox feedback loop between the MCT and myofibers maintains the dynamic developmental homeostasis between muscle components while also regulating MCT organization. Our results allow a better understanding of diseases such as Duchenne muscular dystrophy, in which LOX and TGFβ signaling have been implicated and the balance between muscle constituents is disturbed.

KEY WORDS: TGF-beta, Collagen, Lysyl oxidase, Muscle, Muscle connective tissue, Mouse

INTRODUCTION

Tissue development depends on orchestrated signaling and crosstalk between the constituent cell types. This crosstalk is required for the synchronization and balancing of several processes, including regulation of the relative amounts of the distinct components that make up the tissue and, largely in parallel, for the regulation of their spatial organization. However, how these processes are regulated and coordinated *in vivo* has largely remained unclear. Skeletal muscle, the largest tissue in the human body constituting up to 40-50% of total body mass, is an integrated tissue mainly composed of myofibers, fibroblasts, extracellular matrix (ECM) and satellite cells (SCs), among others (Gray et al., 2005). While much is known about the transcriptional programs generating each cell type, how these cells interact to yield a functional muscle has received less attention and remains unclear.

Muscle connective tissue (MCT), which is rich in a mixture of fibroblasts and the ECM components proteoglycans and collagen fibers, is intimately linked with the muscles. It sheathes the muscle fibers, fasciculi and muscle (Gray et al., 2005), as well as the tendons. Disruption of MCT integrity, organization or composition affects myogenic progenitor specification, differentiation, patterning, morphogenesis and regeneration (Grim and Wachtler, 1991; Kardon et al., 2003; Hasson et al., 2010; Mathew et al., 2011; Murphy et al., 2011), demonstrating that crosstalk between these muscle components plays a cardinal role during myogenesis. However, the molecular signals involved and the ECM molecules carrying out these activities have remained largely unknown (Hasson, 2011).

A key signaling pathway affecting both MCT and myogenesis is the transforming growth factor β (TGFβ) cascade (Shi and Massagué, 2003), which has been shown to induce ECM deposition and MCT fibroblast proliferation but also to inhibit myogenic differentiation (Heino and Massague, 1990; Cusella-De Angelis et al., 1994; Liu et al., 2004; Burks and Cohn, 2011). Members of the TGFβ family are expressed in the MCT during distinct myogenic stages and directly affect both myoblasts and MCT fibroblasts (McLennan, 1993).

The main extracellular components of connective tissues and the MCT belong to the collagen superfamily (Sasse et al., 1981; Myllyharju and Kivirikko, 2004). More specifically, collagen type I (ColI) is the most abundant protein in the vertebrate body and the main extracellular component of the MCT (Sasse et al., 1981; Myllyharju and Kivirikko, 2004). Following translation, collagen molecules undergo several post-translational modifications that facilitate their crosslinking and consequently the formation of collagen fibers. A key enzyme in this process is lysyl oxidase (Lox), a copper-dependent extracellular amine-oxidase that initiates the lysine- and hydroxylysine-derived crosslinking of fibrillar collagen molecules such as ColI (Csiszar, 2001; Myllyharju and Kivirikko, 2004; Mäki, 2009). Recent studies have shown that, in addition to its primary identified targets, the fibrillar collagens and elastin, Lox can oxidize and affect the activity of a growing number of proteins, including cytokines and membrane receptors (Csiszar, 2001; Jeay et al., 2003; Kagan and Li, 2003; Atsawasuwan et al., 2008; Lucero et al., 2008, 2011).

ECM organization and collagen fiber formation are implicated in muscular diseases but their contribution to embryonic myogenesis has not been rigorously addressed. To directly examine the resulting effects on myogenesis we have analyzed *Lox* mutant ($Lox^{-/-}$) mice (Mäki et al., 2002), in which defects in collagen fiber crosslinking lead to a disruption of ECM organization. We find that in these mice the homeostatic balance between myofibers and MCT (ECM and fibroblasts) is abrogated. Thus, $Lox^{-/-}$ muscles contain fewer myofibers but have an excess of MCT fibroblasts and ColI deposition. Furthermore, the deposited collagen fibrils are disorganized. We further find that Lox secreted from the myofibers attenuates TGFβ signaling in the MCT, and that in $Lox^{-/-}$ muscles this cascade is excessively activated. Our work uncovers a feedback mechanism between the distinct muscle

[1]The Rappaport Faculty of Medicine and Research Institute, Technion – Israel Institute of Technology, Haifa 31096, Israel. [2]Oulu Center for Cell-Matrix Research, Biocenter Oulu and Faculty of Biochemistry and Molecular Medicine, University of Oulu, Oulu 90220, Finland. [3]Department of Biological Regulation, The Weizmann Institute of Science, Rehovot 76100, Israel. [4]Biocenter Oulu and Department of Pathology, University of Oulu and Oulu University Hospital, Oulu 90220, Finland.
*These authors contributed equally to this work

‡Author for correspondence (phasson@tx.technion.ac.il)

Received 28 May 2014; Accepted 13 January 2015

Development (2015) 142, 983-993 doi:10.1242/dev.113449

components that ensures that a dynamic homeostatic balance between the amount of myofibers and MCT is maintained. Notably, a consequence of this feedback loop is the synchronization of ECM deposition together with its maturation and post-translational organization, facilitating the development of a functional and properly patterned tissue.

RESULTS

Lox activity is required for normal myofiber development

Lox$^{-/-}$ mice die upon birth due to cardiovascular and respiratory system abnormalities that lead to aortic aneurysms and to occasional rupturing of the diaphragm (Mäki et al., 2002, 2005; Hornstra et al., 2003), primarily caused by ECM organization defects in these tissues (Warburton and Shi, 2005). Further, Lox knockdown in the zebrafish embryo disturbed somite development, although this was attributed to disruption of the adjacent tissue, the notochord, a regulator of somite organization (Reynaud et al., 2008). Together, these observations suggest that Lox participates in muscle development, although the underlying mechanism is unknown. To directly test whether Lox contributes to muscle development, we harvested *Lox*$^{-/-}$ pups immediately after birth [postnatal day (P) 0] and analyzed their limb skeletal muscles by whole-mount immunostaining of myosin heavy chain (MHC) to mark the myofibers.

We find that the muscles, most notably (although not exclusively) those of the zeugopod, are shorter, smaller, have a reduced amount of myofibers and are abnormally patterned (Fig. 1A-G; supplementary material Fig. S1A). Although the internal sarcomeric structure of the muscle is grossly normal (supplementary material Fig. S2) and muscles undergo differentiation and myotubes fuse to form muscle bundles, the muscles that form in these mutant limbs are of incorrect size and shape, undergo abnormal splitting, and insert at the wrong locations. Owing to the muscle patterning defects, assigning the specific muscles in the mutants is impossible. However, muscles located at the position where the extensor carpi radialis (ECR) normally resides are ~42% (n=7) of normal length (n=15). Likewise, muscles located at the position of the extensor digitorum communis (EDC) are ~36% (n=7) of the length of the wild-type counterpart (n=15) (Fig. 1). Recently, muscle contraction was shown to be essential for the translocation of the flexor digitorum superficialis (FDS) muscle that originates in the paw and translocates to the forearm during fetal development (Huang et al., 2013). In all mutants examined (n=10), we find that the FDS muscle has not properly translocated to its final position (Fig. 1D, arrowhead). These observations suggest that in *Lox*$^{-/-}$ embryos muscles are not only of the wrong shape and size, but they are also not properly contracting.

Such muscle morphogenesis defects could be caused by defective skeletal patterning, especially since the bones are rich in fibrillar collagens and therefore affected by Lox activity. To test whether these muscle phenotypes are caused by skeletal patterning defects, we stained skeletal preparations of P0 neonates with Alcian Blue and Alizarin Red to reveal cartilage and bone formation, respectively. We find that, in agreement with previous observations, the overall shape and length of the bones as well as the tendon attachment processes are unaffected (supplementary material Fig. S3, arrow and arrowheads) (Pischon et al., 2009). Altogether, these results suggest that the observed muscle phenotypes are not secondary to skeletal patterning defects.

To better characterize the myofiber defects in the mutant muscles, we sectioned *Lox*$^{-/-}$ and control littermate limbs and performed morphometric analyses of the myofibers. We found a significant

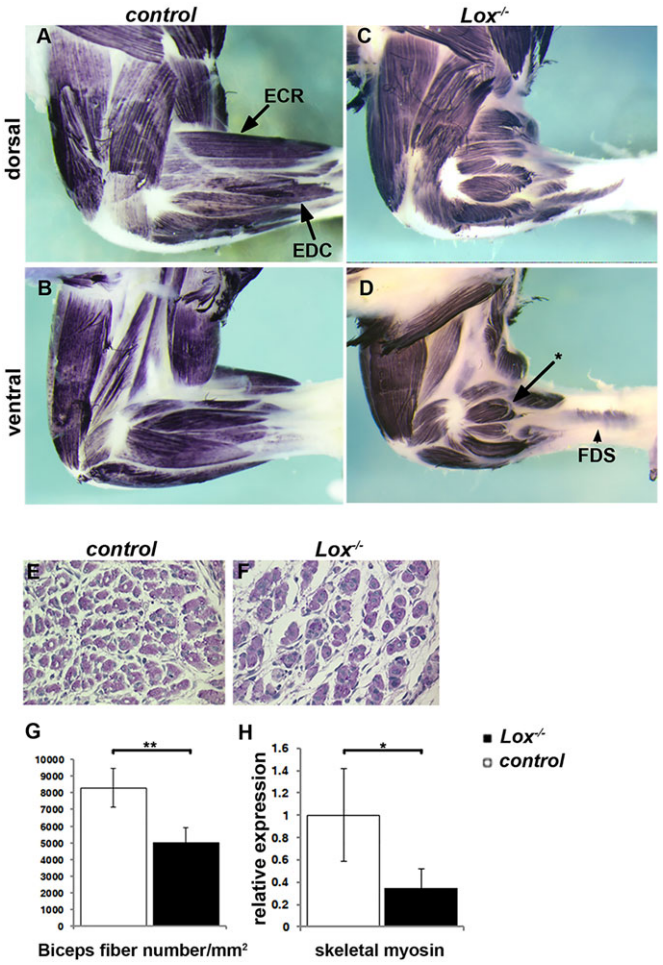

Fig. 1. *Lox*$^{-/-}$ limbs exhibit reduced myofiber content. (A-D) Whole-mount MHC staining of P0 neonates reveals shorter, smaller and mispatterned muscles in *Lox* mutant mice. Arrowhead in D indicates mislocalized flexor digitorum superficialis (FDS) muscle. Arrow with asterisk indicates abnormal muscle splitting. EDC, extensor digitorum communis; ECR, extensor carpi radialis. (E,F) Periodic acid-Schiff staining shows fewer myofibers in *Lox*$^{-/-}$ deltoid muscle, surrounded by a large amount of limb mesenchyme. (G) Morphometric analysis (wild type, n=5; *Lox*$^{-/-}$, n=4) demonstrates fewer myofibers in *Lox*$^{-/-}$ biceps. (H) Western blot analysis of control (n=6) and *Lox*$^{-/-}$ (n=6) E18.5 limb muscles shows a significant decrease in MHC content in the mutant. Data represented are mean±s.d. *P<0.05, **P<0.01.

reduction in the number of myofibers (Fig. 1E-G), but no significant difference in fiber diameters and overall shape between the two genotypes (supplementary material Fig. S1B). To quantify the reduction in myofiber mass, we performed western blot analysis of limb muscles at embryonic day (E) 18.5, which revealed a significant reduction in the MHC content of the limb (Fig. 1H). Altogether, these data demonstrate that Lox activity is required for normal myofiber development.

MCT is impaired and excessively deposited in *Lox* mutant muscles

The myofibers are sheathed by layers of MCT rich in fibroblasts and ECM. This MCT has been shown to intimately interact with and participate in numerous processes affecting developmental and regenerative myogenesis, such as myoblast and SC proliferation, differentiation and patterning (Kardon et al., 2003; Hasson et al., 2010; Mathew et al., 2011; Murphy et al., 2011). Moreover, in muscular dystrophies, such as Duchenne muscular dystrophy

Development (2015) 142, 983-993 doi:10.1242/dev.113449

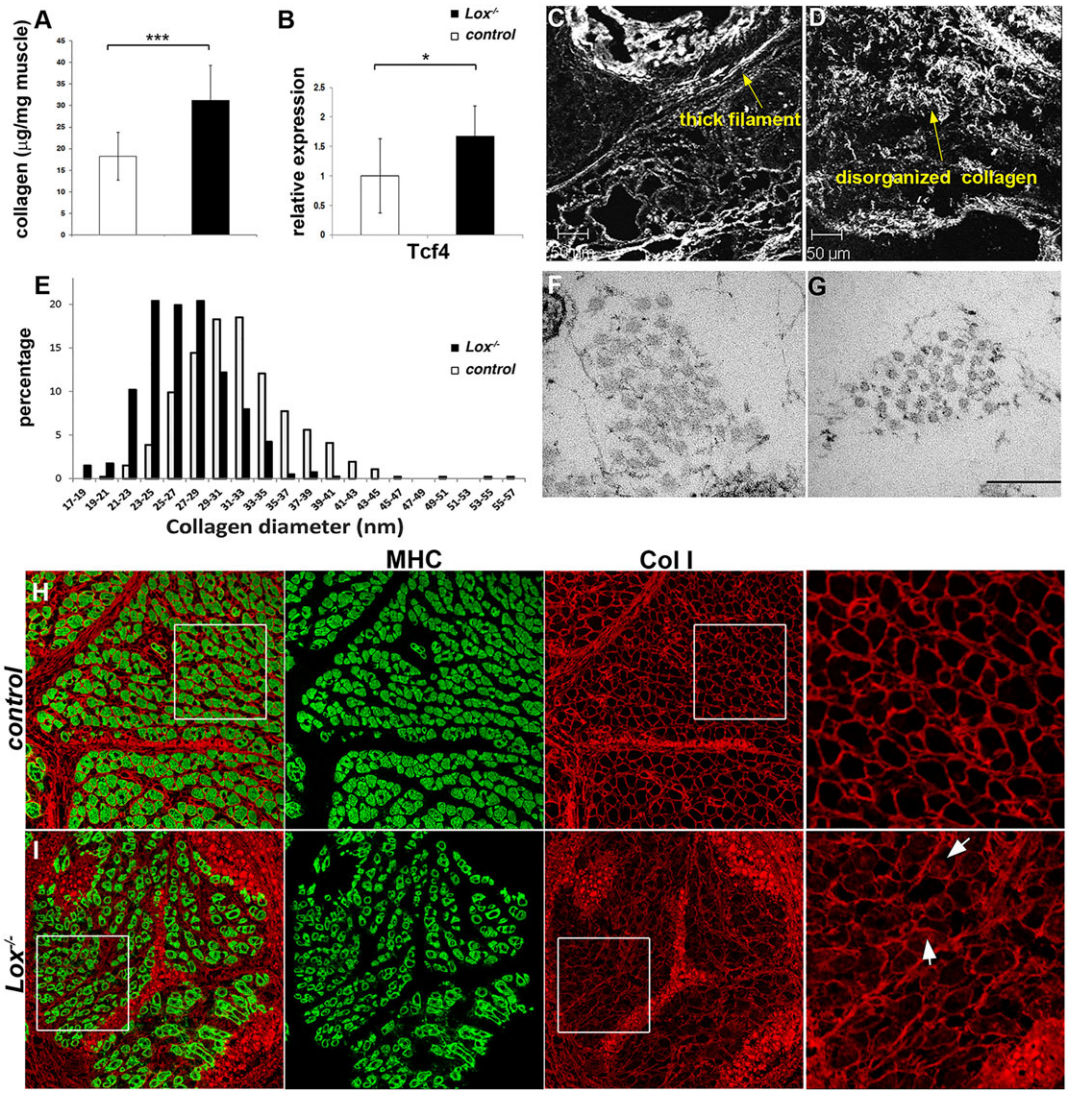

Fig. 2. MCT is upregulated and disorganized following *Lox* deletion. (A) Hydroxyproline assay from E18.5 control (n=14) and $Lox^{-/-}$ (n=11) muscles demonstrates elevated collagen levels in mutants. (B) Western blot analyses from E18.5 control (n=9) and $Lox^{-/-}$ (n=7) forelimbs for Tcf4 demonstrate 67% upregulation in the amount of this MCT marker in the mutant. Data represented are mean±s.d. *P<0.05, ***P<0.001. (C,D) Second harmonic generation for label-free imaging of collagen in the ECM surrounding muscle fibers of wild-type (C) and $Lox^{-/-}$ (D) tissues demonstrates thinner and disorganized collagen following *Lox* deletion. (E) Quantification of collagen fibers using TEM reveals a shift in the width of ColI fibers from thick to narrow in mutant muscles (P<0.001). (F,G) TEM images of ColI fibers from wild-type (F) and $Lox^{-/-}$ (G) muscles. (H,I) Immunofluorescent staining of control (H) and $Lox^{-/-}$ (I) muscles shows ColI (red) sheathing the myofibers (green) is disorganized in mutant muscles (arrows). Boxed regions are magnified to the right. Scale bars: 50 μm in C,D; 200 nm in F,G.

(DMD), muscle fibrosis occurs and excess fibrous ECM is deposited at the expense of the myofibers. This excessive deposition of ECM strongly affects muscle physiology and regeneration, further demonstrating the crucial role played by the MCT in its correct proportion (reviewed by Serrano et al., 2011).

Following the deletion of *Lox* and the associated reduction in myofibers, we could envisage three main scenarios with respect to MCT levels. First, a concomitant reduction of MCT would be observed and the balance between myofibers and connective tissue will be maintained. Second, although myofibers are reduced in the $Lox^{-/-}$ muscles, the amount of MCT would not be affected and thus the two processes would be uncoupled. A third option is that excess MCT will be formed at the expense of the reduced myofibers. To determine which of these options prevails we tested whether any components of the MCT (i.e. fibroblasts and ECM) were affected by the loss of *Lox*. Western blot analysis was used to quantify the amounts of MCT fibroblasts (Tcf4-positive cells; Kardon et al., 2003) and the hydroxyproline assay to quantify the amount of collagens, the main ECM proteins in the MCT (Bailey et al., 1979; Sasse et al., 1981). Notably, and in contrast to the myofibers, we observed a significant increase of 71% and 57% in both the ECM and fibroblast markers, respectively, in E18.5 limb muscle lysates (Fig. 2A,B).

As Lox is a key collagen regulator, we assessed the consequences of its deletion on collagen organization. The second harmonic generation (SHG) technique, which allows label-free imaging of collagen fibers at high resolution on native tissue (Fritzky and Lagunoff, 2013), was used to detect changes in collagen morphology. In the *Lox* mutant muscles, not only are the levels of ColI elevated, but also the normally linear organization of the collagen fibers is disorientated and disrupted (Fig. 2C,D). These defects were verified using transmission electron microscopy (TEM). Immuno-EM analysis for ColI demonstrates that although collagen fibers are present in the muscle (supplementary material

Development (2015) 142, 983-993 doi:10.1242/dev.113449

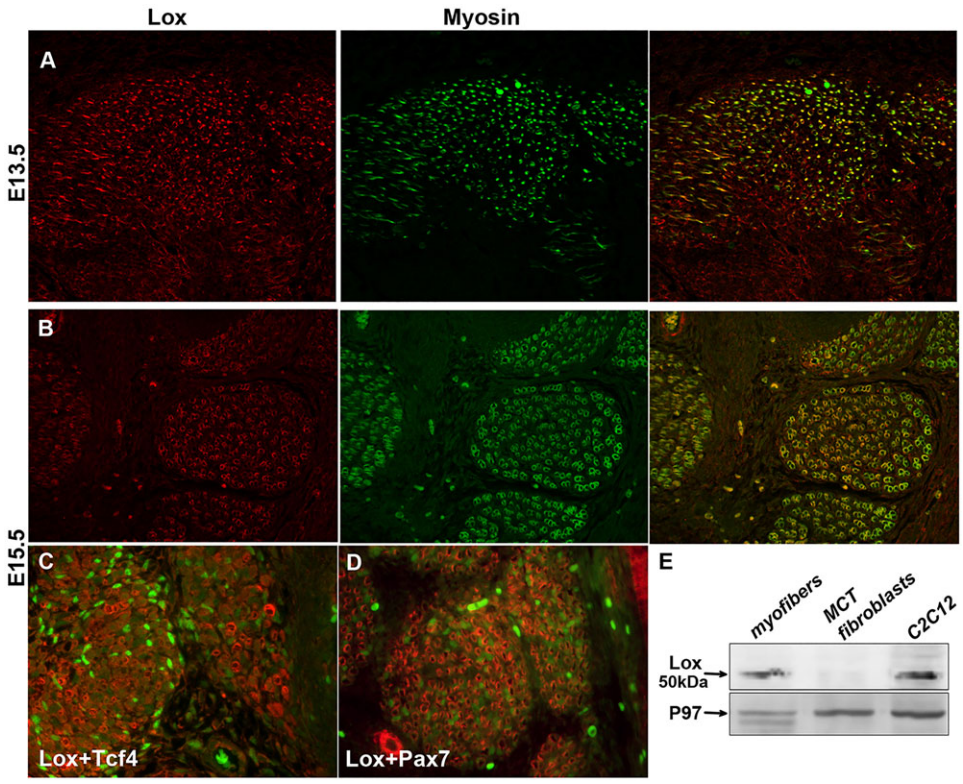

Fig. 3. Lox is expressed in myofibers. (A,B) Immunostaining for Lox (red) and skeletal myosin (A4.1025; green) at E13.5 (A) and E15.5 (B). Note the broader expression of Lox at E13.5 (A), yet by E15.5 Lox muscle expression is restricted to the myofibers (B). (C,D) Immunostaining for Lox (red) and Tcf4 (green, C) or Pax7 (green, D) at E15.5 reinforces that Lox primary expression is not within MCT fibroblasts (C) or myoblast progenitors (D). (E) Western blot analysis from lysates of primary myofibers, primary MCT fibroblasts and the myogenic cell line C2C12 validates Lox expression in myogenic cells and further demonstrates weak Lox expression in these fibroblasts.

Fig. S4A,B), presumably in part due to the expression of other members of the family and to the upregulation of Loxl1 and Loxl3, their organization is impaired (supplementary material Fig. S4C-E). TEM further allowed us to measure the width of the collagen fibers in both genetic backgrounds. In accordance with the results obtained by SHG imaging, we find a shift in the mean width of the collagen fibers in *Lox* mutant muscles, where the thick fibers are largely missing and more thin fibers are detected (Fig. 2E-G).

Both the myofibers and the MCT fibroblasts have been shown to contribute to the ECM of developing muscles (e.g. Bailey et al., 1979; Sasse et al., 1981; Mathew et al., 2011), although the proportional input of each cell type is not clear. Accordingly, we find that both C2C12 cells, a myogenic cell line (Yaffe and Saxel, 1977), and SCs secrete ColI (data not shown). Confocal microscopy of P0 sectioned forelimb zeugopods demonstrate that in the wild-type control muscles ColI forms a lattice sheathing the fibers (marked by MHC, green) and internal ColI staining can be seen in ~20% of the fibers. By contrast, in the mutant limbs, this organized lattice is lost and ColI is also found within more than 70% of the fibers (Fig. 2H,I, arrows), suggesting that the myofibers might be contributing to the excessive ECM secretion. Notably, the dysregulation of ColI is specific, as another member of the collagen superfamily, collagen type IV (ColIV), which is also expressed in muscles yet has not been shown to be a direct substrate for Lox, is not affected in the *Lox* mutant muscles (supplementary material Fig. S5).

Lox expression in embryonic limb development

Lox$^{-/-}$ mice die upon birth, demonstrating that Lox plays an important role during embryonic development; however, its embryonic expression and activities have hardly been examined. To identify the underlying mechanisms of its muscle-related activities, we first characterized its expression pattern. Whole-mount RNA *in situ* hybridization was used to examine *Lox* expression at different stages of embryonic limb development. We compared *Lox* expression with that of markers of the muscular system, namely *Tcf4* marking the MCT fibroblasts (Kardon et al., 2003), *MyoD* (*Myod1*) marking myoblasts (Davis et al., 1987) and *Scx* marking tendon progenitors (supplementary material Fig. S6) (Schweitzer et al., 2001). This analysis revealed that *Lox* expression is first observed in the center of the nascent limb bud at E11.5. Its expression then expands and spans most of the limb abutting the autopod (supplementary material Fig. S6A). The early expression in the proximal domains of the limb is reminiscent of that of the other markers (supplementary material Fig. S6B-D). By E12.5-13.5, when individual muscles become apparent, *Lox* expression resembles (although is less defined than) the *MyoD* expression pattern (supplementary material Fig. S6C).

Lox is expressed in differentiated myofibers

The RNA *in situ* hybridization analysis demonstrates that *Lox* expression temporally and spatially coincides with muscle development (supplementary material Fig. S6), reinforcing the notion that it plays a role in this process. However, this analysis cannot differentiate between the distinct cell types in the growing muscle. To obtain cellular resolution of Lox expression we raised an antibody against a Lox peptide previously shown to specifically recognize the active site within the enzyme (supplementary material Fig. S7) (Erler et al., 2006). Limbs at distinct embryonic stages were sectioned and subjected to double immunohistochemistry analysis using the anti-Lox antibody together with markers of myofibers (MHC), MCT fibroblasts (Tcf4) or myoblast progenitors (Pax7). Coinciding with *Lox* RNA expression at E13.5 (supplementary material Fig. S6), we found that Lox is expressed in a broad area including MHC-expressing cells (Fig. 3A). By E15.5, its expression is restricted to MHC-expressing myofibers within the developing muscle (Fig. 3B). Notably, we did not observe strong Lox

Development (2015) 142, 983-993 doi:10.1242/dev.113449

expression in Tcf4-positive MCT fibroblasts, and no Pax7-expressing myoblast progenitors expressed Lox (Fig. 3C,D).

To strengthen and verify these findings we performed western blot analysis using the Lox antibody and a lysate of primary cultured myofibers generated from SCs, primary MCT fibroblasts and from differentiated fibers derived from the C2C12 murine myoblast cell line. Whereas very weak Lox expression was observed in the MCT fibroblast cells, robust Lox expression was detected in primary and C2C12-derived myofibers (Fig. 3E). We therefore conclude that, during embryonic and fetal myogenesis, Lox is primarily expressed by the differentiated myofibers within the developing muscle.

Lox affects fetal but not embryonic myogenesis

Myogenesis is a multistep process comprising four successive stages (Murphy and Kardon, 2011). In the limb, embryonic myogenesis begins at E10.5 and ends at E12.5-13.5. During this early stage of muscle development, primary myofibers are formed from the progenitor population residing in the limb. To test whether Lox affects embryonic myogenesis we harvested embryos at the end of this stage (E13.5) and subjected them to whole-mount RNA *in situ* hybridization analysis using the muscle markers myogenin (*Myog*) and *MyoD*. Surprisingly, we could not detect any difference in the expression of these markers between $Lox^{-/-}$ and control littermates (Fig. 4A,B; data not shown).

Following embryonic myogenesis, a second wave begins. This wave, termed fetal myogenesis, begins at ∼E14.5 and continues until birth. During this period new muscle fibers form based on the template formed by the primary fibers. Proliferation and differentiation processes are robust and muscle mass increases dramatically (Murphy and Kardon, 2011). To test whether Lox influences fetal myogenesis, we analyzed limbs harvested at E14.5-16.5 (early to mid-fetal myogenesis) from $Lox^{-/-}$ and control littermate embryos (Fig. 4; supplementary material Fig. S8; data not shown). Whole-mount immunostaining with an antibody against fast MHC (My32) reveals that muscle defects are first observed at E16.5. Thus, by mid-fetal myogenesis muscles are shorter, mispatterned and their organization is abnormal, resembling the P0 defects (Fig. 4C-F). Section immunostaining for laminin, which marks the myofiber basal lamina, further demonstrates that in $Lox^{-/-}$ fetal muscles myofiber amounts are reduced and internal fiber organization is lost, resulting in fibers of divergent orientation (Fig. 4G,H).

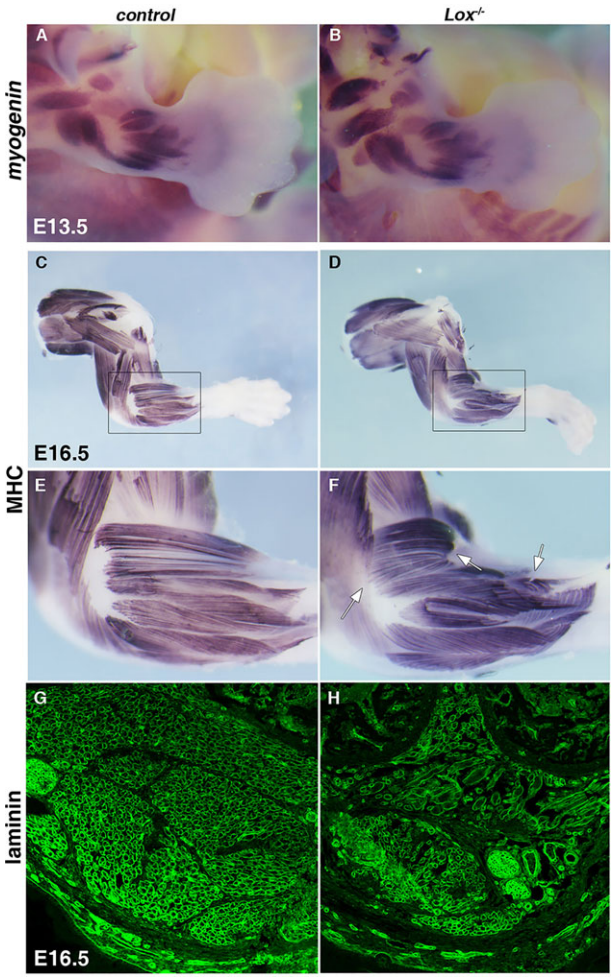

Fig. 4. Lox affects fetal but not embryonic myogenesis. RNA *in situ* staining for myogenin (*Myog*) in control (A) and $Lox^{-/-}$ (B) limbs at E13.5 reveals no difference at this time point. (C,D) MHC (My32) whole-mount immunostaining of E16.5 control and $Lox^{-/-}$ forelimbs shows extensive muscle defects in the mutant embryos. (E,F) Magnification of the boxed regions in C,D showing pattern defects (arrows); muscle insertion points are disrupted and orientation of muscle is abnormal. (G,H) Immunostaining for laminin demonstrates fewer myofibers and loss of internal muscle organization in $Lox^{-/-}$ muscles, where individual fibers assume distinct orientations.

TGFβ signaling is upregulated in $Lox^{-/-}$ muscles

Thus far, our analysis of *Lox* mutant muscles revealed that (1) myofiber content is reduced in the absence of Lox activity (Fig. 1); (2) MCT fibroblasts and ECM deposition are upregulated (Fig. 2); and (3) fetal myogenesis but not embryonic myogenesis is affected in $Lox^{-/-}$ embryos (Fig. 4). All these observations have been associated with augmented TGFβ signaling in muscle and MCT (e.g. Heino and Massague, 1990; Cusella-De Angelis et al., 1994; Liu et al., 2004; Burks and Cohn, 2011).

TGFβ is known to interact with ECM components and this interaction plays an important role in regulating its bioavailability (Hynes, 2009). Lox, being a key regulator of ECM maturation, may thus potentially influence TGFβ activation levels. Furthermore, direct interactions between the two have recently been demonstrated, whereby Lox physically binds mature Tgfβ1. This binding results in an attenuation of TGFβ signaling in a Lox enzyme-dependent manner (Atsawasuwan et al., 2008). Collectively, our observations and the previously published reports on Lox and TGFβ interactions (functional and physical) suggest that alterations in TGFβ signaling could underlie the molecular events that account for the observed *Lox*-dependent muscle phenotypes.

To determine whether Lox affects TGFβ signaling we generated mouse embryonic fibroblasts (MEFs) from control wild-type and from $Lox^{-/-}$ E14.5 embryos and examined whether they respond differently to TGFβ. The MEFs were subjected to short (5-30 min) or long (6-24 h) treatments with various concentrations (0.5-5 ng) of recombinant mouse Tgfβ1. Cells were then lysed and subjected to western blot analysis using phosphorylated (p) Smad2 and Smad3 as a readout of TGFβ signaling. p-Smad2 levels, but not those of p-Smad3, were significantly elevated following TGFβ treatment in $Lox^{-/-}$ MEFs, irrespective of the length of incubation with the cytokine (Fig. 5A; data not shown).

Although p-Smad2 and p-Smad3 are associated with activated TGFβ signaling, whether this ultimately gives rise to a transcriptional response of their target genes is unknown. To test whether the enhancement of p-Smad2 levels in the *Lox* mutant MEFs, and thus the response to TGFβ signaling, is also correlated at the functional transcriptional level, we transfected a reporter

Development (2015) 142, 983-993 doi:10.1242/dev.113449

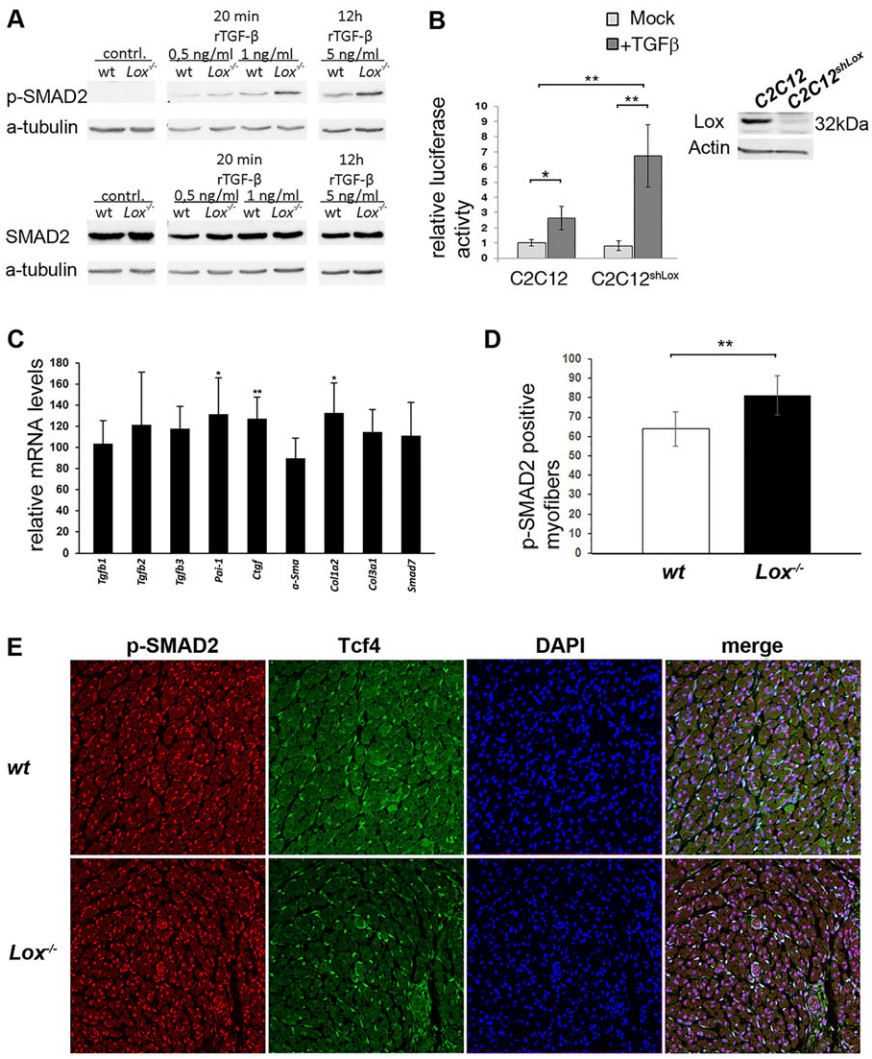

Fig. 5. Lox attenuates TGFβ signaling. (A) MEFs prepared from wild-type (wt) and $Lox^{-/-}$ fetuses were exposed to different amounts of recombinant Tgfβ1 for short and long periods. Western blots for total Smad2 and p-Smad2 were used as a readout of TGFβ activation. *Lox* mutant MEFs show substantially stronger p-Smad2 activation compared with the control. (B) C2C12 cells with reduced *Lox* levels ($C2C12^{shLox}$, right) that were exposed to TGFβ show a significant increase in Smad2/3 signaling as measured by a Smad2/3-responsive luciferase reporter. (C) qRT-PCR analysis of TGFβ transcripts and TGFβ target genes from E18.5 muscles demonstrates a significant upregulation of several targets in $Lox^{-/-}$ muscles. Wild-type expression was set as 100%. (D) Quantification of p-Smad2-positive myofibers in wild type and *Lox* mutant. (E) Examples of p-Smad2 and Tcf4 immunostaining on wild-type and *Lox* mutant E18.5 muscles. Data are represented as mean±s.d. **P*<0.05, ***P*<0.01, ****P*<0.005.

plasmid that contains Smad2/3 binding sites upstream of a luciferase reporter (Cignal). In agreement with the augmented p-Smad2 in *Lox* mutant cells, we observed an increase in luciferase levels in $Lox^{-/-}$ MEFs in comparison with controls (not shown). Altogether, in cells lacking Lox activity the response to TGFβ is greater, demonstrating that Lox inhibits TGFβ-mediated p-Smad signaling.

To test whether this Lox-dependent TGFβ cascade inhibition also takes place in myogenic cells, we took advantage of the C2C12 cell line, which expresses endogenous Lox protein (Fig. 3E). Short hairpin RNA viral particles (MISSION shRNA) were used to generate a stable C2C12 cell line in which Lox levels are significantly reduced ($C2C12^{shLox}$; Fig. 5B). To test if the two cell lines respond differently to TGFβ by activating the cascade's transcriptional program, we transfected the two cell lines with the Cignal reporter (as above) and monitored luciferase activity following application of the growth factor. Eighteen hours following the addition of Tgfβ1, luciferase activity, and hence cascade activation, was >2.5-fold upregulated in comparison to mock (PBS)-treated C2C12 cells, demonstrating their response to the cytokine. Remarkably, in the $C2C12^{shLox}$ cells, activation was >8.3-fold upregulated when compared with the mock-treated cells (Fig. 5B). Overall, these results demonstrate that Lox attenuates TGFβ signaling not only in MEFs but, importantly, also in myogenic cells.

We next examined whether this upregulated TGFβ signaling is observed *in vivo* in the developing *Lox* mutant muscles. We used quantitative RT-PCR (qRT-PCR) to measure TGFβ-regulated target genes, analyzing cDNA prepared from limb muscles of E18.5 wild type and *Lox* mutants. We first defined whether the TGFβ ligands themselves are upregulated in the mutant muscles. We did not find significant upregulation of any TGFβ ligand in the mutant muscles, although *Tgfb2* and *Tgfb3* transcript levels were slightly upregulated. In particular, we found that some TGFβ targets [e.g. those genes encoding PAI-1 (*Serpine1*), Ctgf and ColI (*Col1a2*), but not α-SMA (*Acta2*), ColIII (*Col3a1*) or Smad7] were significantly upregulated (~30%) in *Lox* mutant muscles (Fig. 5C).

The above results demonstrate that Lox attenuates TGFβ signaling *in vivo*; however, it does not differentiate which cells within the muscle (myogenic or MCT fibroblasts) are mostly affected. To examine whether Tcf4-positive MCT fibroblasts, myogenic cells or both upregulate TGFβ signaling following *Lox* deletion, we immunostained E18.5 limb muscle sections from wild type (n=9) and $Lox^{-/-}$ (n=7) for p-Smad2 and Tcf4. We found that p-Smad2 levels are significantly elevated in the nuclei of myogenic cells and also tend to be so in Tcf4-positive MCT fibroblasts (Fig. 5D,E; data not shown). In summary, we conclude that TGFβ signaling is enhanced in muscles devoid of Lox.

Although the above assays demonstrate that Lox activity regulates TGFβ signaling, additional modes of interaction have been suggested to take place. Thus, during angiogenesis Lox was placed downstream of TGFβ signaling and the activation of the pathway leads to its

Development (2015) 142, 983-993 doi:10.1242/dev.113449

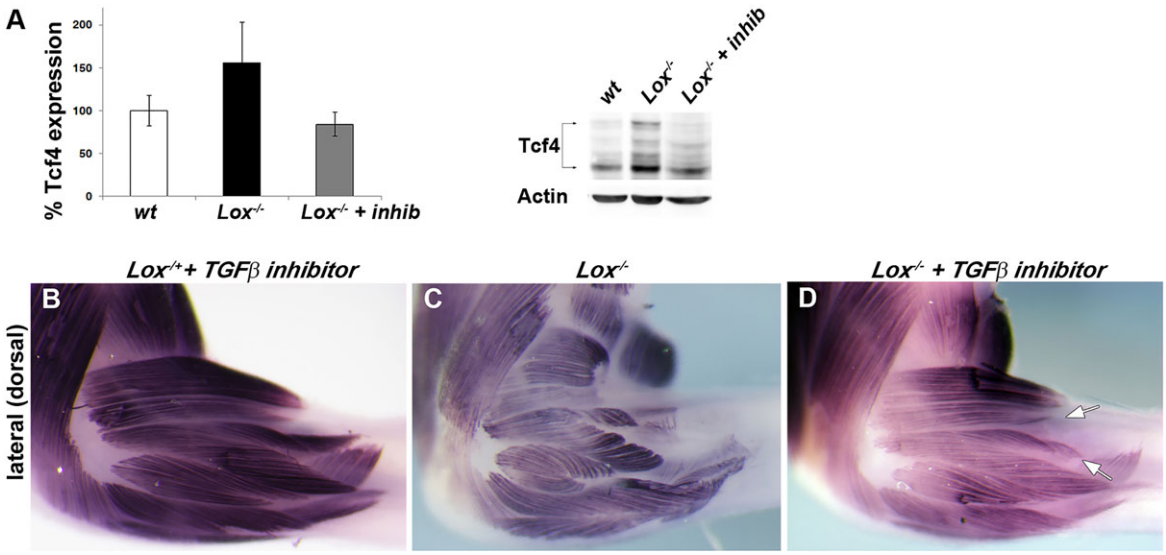

Fig. 6. *Lox*-dependent muscle phenotype is rescued by TGFβ cascade inhibition. (A) Western blot analysis reveals that elevated Tcf4 expression in $Lox^{-/-}$ muscles is rescued by TGFβ inhibition (n=3). (B-D) MHC (My32) whole-mount immunostaining of $Lox^{-/+}$ (B) and $Lox^{-/-}$ (C,D). Muscle defects are not observed following inhibition of TGFβ in the heterozygous embryos (B). The *Lox*-dependent muscle phenotypes observed at E16.5 are greatly reduced following TGFβ signal inhibition (compare C with D). Arrows in D indicate some of the defects still observed in the 'TGFβ-rescued' embryos.

transcriptional upregulation (e.g. Gacheru et al., 1997). In addition, Smad4, a downstream effector of the TGFβ/BMP pathway, was shown to directly bind and regulate the *Lox* promoter (Salazar et al., 2013). Could similar regulation of Lox by TGFβ occur in the developing embryo? To test this possibility, we took advantage of the developing chick limb. Beads soaked with either Tgfβ1 or Tgfβ2 were implanted in lateral plate mesoderm at presumptive regions of the future forelimbs (HH stage 16) and following 2 days of incubation the chicks were harvested and *in situ* stained for chick *Lox* expression. A significant increase in *Lox* expression was observed following TGFβ administration as compared with the PBS-treated bead (supplementary material Fig. S9), indicating that TGFβ-Lox transcriptional regulation also takes place during development.

TGFβ inhibition rescues the $Lox^{-/-}$ muscle phenotype

Our results thus far are indicative of myofiber-secreted Lox that represses TGFβ signaling in the muscle. We presume that, in the absence of Lox, which acts as a TGFβ activity repressor, augmented activation of the cascade leads to the observed myofiber and MCT defects. To test this hypothesis, we aimed to attenuate the cascade *in vivo* to see whether this would rescue the *Lox*-related MCT and muscle defects. Pregnant mice were injected at E12.5 and E13.5 (the onset of robust *Lox* expression) with 25 ng TGFβ receptor I antagonist (Li et al., 2006), which inhibits the receptor by preventing signal propagation. In many instances this injection regime resulted in embryonic lethality and hemorrhages were observed in the harvested embryos. Strikingly, the vast majority of the surviving embryos were either homozygous or heterozygous *Lox* mutants; hardly any wild-type embryos survived this TGFβ inhibition regime. To overcome this lethality, we harvested the embryos at E16.5, which is the earliest time point by which a clear muscle phenotype could be monitored in the $Lox^{-/-}$ embryos. To test whether TGFβ inhibition would reduce the augmented levels of MCT fibroblasts in *Lox* mutant muscles, we lysed the muscles and carried out a western blot analysis using Tcf4 antibody. Notably, we found that TGFβ inhibition is able to reduce Tcf4 to normal levels even in the absence of *Lox* (Fig. 6A).

The above results suggest that many of the muscle-related defects observed in $Lox^{-/-}$ mice are caused by augmentation of TGFβ. To test whether inhibition of the signal would also rescue muscle amount and lead to an attenuation of muscle patterning defects (e.g. Figs 1 and 4), we harvested embryos and analyzed them by whole-mount My32 immunostaining. Strikingly, $Lox^{-/-}$ limbs (n=7 out of 8) from embryos that had received the TGFβ inhibitor showed a dramatic rescue of the abnormal $Lox^{-/-}$ muscle phenotype and demonstrated only mild muscle defects (Fig. 6B-D; supplementary material Table S2). Altogether, these results strongly indicate that enhanced TGFβ activity is the major cause of the *Lox*-dependent muscle defects.

DISCUSSION

Homeostatic balance of the components of a developing tissue is crucial for its proper development and function. Proper formation of a growing tissue requires both the deposition of the various components and their concomitant organization. How these processes are synchronized and regulated *in vivo* has remained largely unknown. Here we show that an interplay between Lox, a myofiber-secreted enzyme, and TGFβ, a cytokine acting in the MCT on myofibers and fibroblasts to inhibit myogenesis and promote MCT development, is at the heart of these dual activities. Our results demonstrate that in mice devoid of Lox the balance between the myofibers and MCT (both ECM and fibroblasts) is abrogated, leading to excessive MCT deposition at the expense of myofibers. Notably, the deposited ECM is disorganized in the absence of Lox activity. We further find that in MEFs, in myogenic cells and in muscles with no or reduced Lox activity, TGFβ signaling is augmented, demonstrating that Lox attenuates the signaling capabilities of this cytokine. Notably, apart from promoting MCT development and inhibiting myogenesis, we find that TGFβ also induces Lox, its negative regulator, thus generating a feedback loop between the two secreted proteins and between the myofibers and MCT. Remarkably, *in vivo* attenuation of TGFβ signaling is able to rescue the *Lox*-dependent muscle phenotypes. Altogether, these results uncover a feedback mechanism whereby

Development (2015) 142, 983-993 doi:10.1242/dev.113449

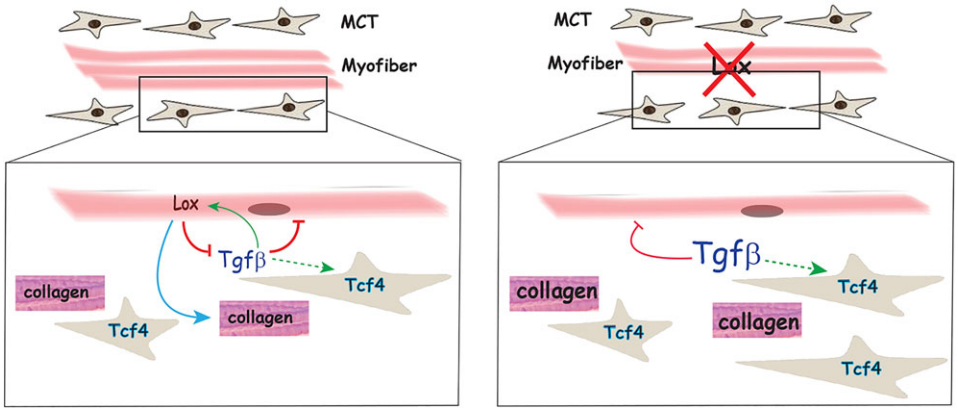

Fig. 7. Model of the Lox-TGFβ feedback loop in developing muscles. (Left) A feedback loop between myofiber-secreted Lox and TGFβ in the MCT regulates the balance between the amounts of MCT versus myofibers. This feedback loop further allows the concomitant synchronization of ECM organization along with its secretion. (Right) In $Lox^{-/-}$ muscles, TGFβ signaling is upregulated leading to excessive MCT deposition but also to a reduction in myofibers and loss of collagen organization.

myofibers regulate the amount of MCT, in terms of both ECM and fibroblasts. In turn, the MCT (via TGFβ) induces the expression of its repressor. That Lox, a key regulator of ECM organization, is at the focal point of this feedback loop allows ECM organization to be orchestrated with the balancing of muscle components during myogenesis (Fig. 7).

How does Lox regulate the TGFβ signaling cascade? A recent report by Atsawasuwan has demonstrated that Lox physically binds Tgfβ1 (Atsawasuwan et al., 2008). Although this binding is not dependent on Lox enzymatic activity, the attenuation of downstream signaling is dependent on the oxidation capabilities of Lox. Could there be other forms of regulation? Notably, TGFβ is secreted as an inactive complex. Following its secretion, the complex binds latent TGFβ-binding protein (LTBP). TGFβ becomes incorporated into the ECM through interactions of LTBP with a number of ECM components, including collagen and fibronectin (Rifkin, 2005). Indeed, mutations in structural components of the ECM lead to dysregulated activation of TGFβ signaling (e.g. Neptune et al., 2003). Furthermore, disruption of the ECM in bone fracture, ligament truncation or skeletal muscle injury leads to an excess release of latent TGFβ from the ECM resulting in ectopic signaling activity that ultimately leads to delayed healing and massive cell death (e.g. Maeda et al., 2011). Upon loss of Lox, the inefficient crosslinking of collagens (and elastin) reduces their tensile strength and increases their solubility, rendering them highly susceptible to proteolysis, which could result in elevated amounts of TGFβ in the tissue. Indeed, in *Lox* mutant muscles organization of the ECM is strongly affected (e.g. Fig. 2), raising the possibility that, apart from Lox-mediated oxidation of the cytokine, additional modes of regulation might lead to excessive TGFβ signaling. The fact that addition of a recombinant TGFβ protein (and not the propeptide with its latency-associated peptide) resulted in enhanced activation of p-Smad2 in cell culture suggests that, in this scenario, Lox either acts directly at the level of the recombinant TGFβ (e.g. via oxidation of the ligand) or at the level of its receptor, and independently of altered ECM organization. Notably, activation of the pathway in C2C12 cells also occurred with recombinant Tgfβ2. Here, too, loss of *Lox* led to an increase in reporter signal. Mature Tgfβ1 and Tgfβ2 are more than 70% identical and the lysine residues in the basic C-terminal part of these cytokines, which is the domain suggested to be bound by Lox (Atsawasuwan et al., 2008), are conserved. Thus, it remains possible that Lox oxidizes and inhibits Tgfβ2 as well, which, like Tgfβ1, is expressed during myogenesis (Saxena et al., 2007). Further experiments are required to test whether the *in vivo* muscle phenotypes are mediated by Lox oxidation of TGFβ or whether additional mechanisms are at work.

One of the major contributors to neonatal $Lox^{-/-}$ lethality is aortic aneurysms. Analysis of these aneurysms reveals defects in the medial layer of the vessel, characterized by a discontinuous smooth muscle cell layer (Mäki et al., 2002). Likewise, TGFβ has also been shown to be a key player in medial smooth muscle cell development, and mutations affecting TGFβ signaling are associated with connective tissue disorders affecting the vasculature (e.g. Marfan syndrome and hereditary hemorrhagic telangiectasia). Our data suggest that Lox attenuates TGFβ signaling in developing muscles. Indeed, TGFβ inhibition was able to rescue to a large extent the Lox-dependent muscle defects (Fig. 6). Interestingly, however, when the 'TGFβ-inhibited' embryos were harvested, numerous hemorrhages were observed in $Lox^{-/-}$ embryos at earlier stages and in larger quantities than normally observed in these mutant embryos (not shown). These observations suggest that, at least in the developing vessels, the interplay between Lox and TGFβ is acting differently than during myogenesis. Why should there be a difference between the Lox-TGFβ interplay in the two tissues, especially since both are expressed in and regulate processes affecting endothelial and smooth muscle cells as well as the sheathing adventitial fibroblasts? An attractive and likely possibility is that the difference lies in the sensitivity of the two tissues to TGFβ signaling. Nonetheless, our results suggest that Lox attenuates TGFβ signaling at the level of the receptor or upstream. Whereas myogenic cells express both types of TGFβ receptor type I, namely Alk1 (Acvrl1) and Alk5 (Tgfβr1) (Luo et al., 2010), endothelial cells express Alk1 whereas smooth muscle cells express Alk5 (Seki et al., 2006). Furthermore, Alk1 has been shown to mainly activate the Smad1/5 pathway, whereas Alk5 activates the Smad2/3 pathway. Thus, it is possible that Lox can differentially oxidize only one receptor or that an oxidized TGFβ is less active upon binding to one but not the other receptor. As a result, inhibition of TGFβ in the background of a *Lox* mutant embryo would differentially inhibit endothelial and smooth muscle cell TGFβ signaling.

Pathological alterations in MCT activities or in its equilibrium within the muscle can lead to muscular dystrophies (MD), a group of muscle disorders mostly characterized by progressive skeletal muscle weakness and degeneration. The most common type of MD, affecting 1:3500 live male births, is DMD. Common symptoms of DMD include progressive muscle weakness and muscle wasting resulting in a shortened life expectancy, usually below the early 30s. In DMD, as well as in other MD, muscle regeneration becomes less effective and instead an excess deposition of connective tissue takes place (fibrosis). This fibrotic reaction directly causes muscle dysfunction and

Development (2015) 142, 983-993 doi:10.1242/dev.113449

contributes to the lethal phenotype of DMD and other related MD. The underlying mechanisms regulating this fibrotic reaction are poorly understood, although ectopic activation of the TGFβ signaling pathway, at least in part due to proteolysis of the ECM, has been demonstrated to contribute to this pathology (reviewed by Burks and Cohn, 2011). Fibrotic hearts and muscles from DMD patients and *mdx* mice, which are mutant for dystrophin as the murine model for DMD, ectopically express Lox (Spurney et al., 2008; Desguerre et al., 2012), and *Lox* has been suggested to be one of the core genes leading to the DMD phenotype (Ichim-Moreno et al., 2010). Recent work has demonstrated that blocking the activity of LOXL2, a Lox family member, is able to stop and even reduce lung and liver fibrosis (Barry-Hamilton et al., 2010), suggesting that Lox enzymes are bona fide targets for the development of anti-fibrotic treatments. Muscle development and regeneration share many similarities. Thus, understanding the roles of Lox during embryonic muscle development will be crucial towards our understanding of its activities in muscle fibrosis.

MATERIALS AND METHODS

Mouse embryos

All experiments involving live vertebrates conform to the relevant regulatory standards (institutional and national animal welfare laws, guidelines and policies). Embryonic day was staged according to Kaufmann (1992); noon of the day a vaginal plug was observed was marked as E0.5. *Lox* mutant mice were described previously (Mäki et al., 2002).

Histological analyses

E18.5 embryos were fixed overnight in 10% buffered formalin. Sections were stained with Masson's trichrome and periodic acid-Schiff (PAS) stain. Staining details can be found in the supplementary Materials and Methods.

RNA *in situ* hybridization and immunohistochemistry

Whole-mount RNA *in situ* hybridizations were carried out essentially as previously described (Riddle et al., 1993) using the probes described in the supplementary Materials and Methods. Section and whole-mount immunohistochemistry were carried out essentially as described (Hasson et al., 2010) using the antibodies described in the supplementary Materials and Methods.

Western blotting

Protein lysates harvested from mouse embryonic limbs or MEFs (see supplementary Materials and Methods) were subjected to SDS-PAGE. Gels were transferred to nitrocellulose membranes, which were then probed with the following antibodies: anti-Tcf4 (Millipore; clone 6H5-3, 1:1000); anti-myosin (A4.1025, DSHB; 6H5-3, 1:100); Smad2 (Cell Signaling, 5339, 1:1000), Smad3 (Cell Signaling, 9523, 1:1000), p-Smad2 (Cell Signaling, 3108, 1:1000), p-Smad3 (Cell Signaling; 9523, 1:1000); and Lox (GenScript, raised in rabbits against EDTSCDYGYHRRFA; 1:500). The specificity of the Lox antibody was determined using HEK293 cell lysates that overexpress Lox in comparison to native HEK293 cells; the expected protein sizes (~37 kDa and ~50 kDa) were observed. Equal protein loading was determined using an antibody directed against Psmd2 (Psmd2, 1:3000; kindly provided by Ariel Stanhill, Technion, IL, USA) or actin (MP Biochemicals; clone C4, 1:5000).

Collagen assay

The amount of collagen in forelimb muscles was measured using a hydroxyproline assay (Chondrex) according to the manufacturer's instructions and as outlined in the supplementary Materials and Methods.

Luciferase assay

TGFβ pathway analysis using the Cignal reporter (Qiagen) and Dual-Luciferase Reporter Assay System (Promega) is oulined in the supplementary Materials and Methods.

Two-photon microscopy and second harmonic generation (SHG)

Muscles were imaged using a two-photon microscope located at the *in vivo* imaging unit of the Weizmann Institute: a 2PM:Zeiss LSM 510 META NLO equipped with a broadband Mai Tai-HP-femtosecond single-box tunable Ti-sapphire oscillator, with automated broadband wavelength tuning 700-1020 nm from Spectraphysics, for two-photon excitation. For collagen SHG imaging a wavelength of 800 nm was used (detection at 400 nm), using the ×20 objective.

Transmission electron microscopy

Muscle tissues from E18.5 embryos were fixed with buffer containing 1% glutaraldehyde and 4% formaldehyde in 0.1 M phosphate buffer, post-fixed with 1% osmium tetroxide, dehydrated in acetone and embedded in Epon LX112 (Ladd Research Industries). Thin sections were cut with a Leica Ultracut UCT microtome, stained in uranyl acetate and lead citrate and examined in a Tecnai Spirit transmission electron microscope (FEI). Images were captured with a Quemesa CCD camera (Olympus). Collagen diameters were calculated from the electron microscopy images using ImageJ 1.44p (NIH). Statistical analyses were performed using Student's *t*-tests.

RNA isolation and qRT-PCR

Muscle tissues were dissected from the forelimbs of E18.5 embryos, frozen on dry ice and stored at −70°C until lysate preparation. Total RNA was isolated using TriPure isolation reagent (Roche Applied Science) and further purified with an EZNA total RNA kit (OMEGA Bio-Tek), and reverse transcription was performed with an iScript cDNA synthesis kit (Bio-Rad). qPCR was performed with iTaq Universal SYBR Green Supermix (Bio-Rad) and a CFX96 Touch real-time PCR detection system. Primers are listed in supplementary material Table S1. Quantitect primer assay (Qiagen) was used for *Pai-1* and *Smad7*. Expression levels were normalized to β-actin (*Actb*). Statistical analyses were performed using Student's *t*-tests.

TGFβ inhibition and activation

Pregnant mice were subject to intraperitoneal injection twice, once at E12.5 and once at E13.5, with 25 ng TGFβ receptor I antagonist (Calbiochem, 616451) each day and harvested at the designated day. Activation of TGFβ in chick limb buds is described in the supplementary Materials and Methods.

Lox knockdown using shRNA

Lox knockdown in C2C12 cells was carried out essentially as described in the supplementary Materials and Methods.

Acknowledgements

We thank I. Solomonov for assistance with the SHG analysis; T. Schultheiss and E. Zelzer for critical reading of the manuscript; G. Kardon, E. Bengal and G. Neufeld and members of their labs for helpful discussions; R. Polojärvi, M. Siurua and A. Kokko for technical assistance; and the personnel of the Biocenter Oulu EM Core Facility, which is cofunded by the University of Oulu and Biocenter Finland, and the University of Oulu Laboratory Animal Center for excellent technical assistance.

Competing interests

The authors declare no competing or financial interests.

Author contributions

L.K. and A.L. performed the majority of the experiments. M.G. and I.S. performed and analyzed the SHG analysis; S.S.B. and S.E. participated in cell culture experiments and western blot analyses. P.S. assisted in immunohistochemical analyses. A-H.R. participated in the morphometric analyses. J.M. provided the Lox-deficient mouse line for the study and assisted in writing the manuscript. J.M.M. planned the study with P.H. and assisted with writing the manuscript. R.S. carried out and analyzed the TEM samples.

Funding

P.H. was supported by grants from the Israeli Science Foundation [1072/13], Binational Science Foundation [2011437] and a Rappaport Family Institute Research Grant. J.M. was supported by the Academy of Finland and S. Juselius Foundation. J.M. was supported by an Academy of Finland Center of Excellence 2012-2017 grant [251314].

Supplementary material

Supplementary material available online at
http://dev.biologists.org/lookup/suppl/doi:10.1242/dev.113449/-/DC1

References

Atsawasuwan, P., Mochida, Y., Katafuchi, M., Kaku, M., Fong, K. S. K., Csiszar, K. and Yamauchi, M. (2008). Lysyl oxidase binds transforming growth factor-beta and regulates its signaling via amine oxidase activity. *J. Biol. Chem.* **283**, 34229-34240.

Bailey, A. J., Shellswell, G. B. and Duance, V. C. (1979). Identification and change of collagen types in differentiating myoblasts and developing chick muscle. *Nature* **278**, 67-69.

Barry-Hamilton, V., Spangler, R., Marshall, D., McCauley, S., Rodriguez, H. M., Oyasu, M., Mikels, A., Vaysberg, M., Ghermazien, H., Wai, C. et al. (2010). Allosteric inhibition of lysyl oxidase-like-2 impedes the development of a pathologic microenvironment. *Nat. Med.* **16**, 1009-1017.

Burks, T. N. and Cohn, R. D. (2011). Role of TGF-beta signaling in inherited and acquired myopathies. *Skelet. Muscle* **1**, 19.

Csiszar, K. (2001). Lysyl oxidases: a novel multifunctional amine oxidase family. *Prog. Nucleic Acid Res. Mol. Biol.* **70**, 1-32.

Cusella-De Angelis, M. G., Molinari, S., Le Donne, A., Coletta, M., Vivarelli, E., Bouche, M., Molinaro, M., Ferrari, S. and Cossu, G. (1994). Differential response of embryonic and fetal myoblasts to TGF beta: a possible regulatory mechanism of skeletal muscle histogenesis. *Development* **120**, 925-933.

Davis, R. L., Weintraub, H. and Lassar, A. B. (1987). Expression of a single transfected cDNA converts fibroblasts to myoblasts. *Cell* **51**, 987-1000.

Desguerre, I., Arnold, L., Vignaud, A., Cuvellier, S., Yacoub-Youssef, H., Gherardi, R. K., Chelly, J., Chretien, F., Mounier, R., Ferry, A. et al. (2012). A new model of experimental fibrosis in hindlimb skeletal muscle of adult mdx mouse mimicking muscular dystrophy. *Muscle Nerve* **45**, 803-814.

Erler, J. T., Bennewith, K. L., Nicolau, M., Dornhöfer, N., Kong, C., Le, Q.-T., Chi, J.-T. A., Jeffrey, S. S. and Giaccia, A. J. (2006). Lysyl oxidase is essential for hypoxia-induced metastasis. *Nature* **440**, 1222-1226.

Fritzky, L. and Lagunoff, D. (2013). Advanced methods in fluorescence microscopy. *Anal. Cell. Pathol. (Amst.)* **36**, 5-17.

Gacheru, S. N., Thomas, K. M., Murray, S. A., Csiszar, K., Smith-Mungo, L. I. and Kagan, H. M. (1997). Transcriptional and post-transcriptional control of lysyl oxidase expression in vascular smooth muscle cells: effects of TGF-beta 1 and serum deprivation. *J. Cell. Biochem.* **65**, 395-407.

Gray, H., Standring, S., Ellis, H. and Berkovitz, B. K. B. (2005). *Gray's Anatomy: The Anatomical Basis of Clinical Practice*. Edinburgh: Elsevier Churchill Livingstone.

Grim, M. and Wachtler, F. (1991). Muscle morphogenesis in the absence of myogenic cells. *Anat. Embryol. (Berl.)* **183**, 67-70.

Hasson, P. (2011). "Soft" tissue patterning: muscles and tendons of the limb take their form. *Dev. Dyn.* **240**, 1100-1107.

Hasson, P., DeLaurier, A., Bennett, M., Grigorieva, E., Naiche, L. A., Papaioannou, V. E., Mohun, T. J. and Logan, M. P. O. (2010). Tbx4 and Tbx5 acting in connective tissue are required for limb muscle and tendon patterning. *Dev. Cell* **18**, 148-156.

Heino, J. and Massague, J. (1990). Cell adhesion to collagen and decreased myogenic gene expression implicated in the control of myogenesis by transforming growth factor beta. *J. Biol. Chem.* **265**, 10181-10184.

Hornstra, I. K., Birge, S., Starcher, B., Bailey, A. J., Mecham, R. P. and Shapiro, S. D. (2003). Lysyl oxidase is required for vascular and diaphragmatic development in mice. *J. Biol. Chem.* **278**, 14387-14393.

Huang, A. H., Riordan, T. J., Wang, L., Eyal, S., Zelzer, E., Brigande, J. V. and Schweitzer, R. (2013). Repositioning forelimb superficialis muscles: tendon attachment and muscle activity enable active relocation of functional myofibers. *Dev. Cell* **26**, 544-551.

Hynes, R. O. (2009). The extracellular matrix: not just pretty fibrils. *Science* **326**, 1216-1219.

Ichim-Moreno, N., Aranda, M. and Voolstra, C. R. (2010). Identification of a gene expression core signature for Duchenne muscular dystrophy (DMD) via integrative analysis reveals novel potential compounds for treatment. In 2010 IEEE Symposium on Computational Intelligence in Bioinformatics and Computational Biology (CIBCB), pp. 1-6.

Jeay, S., Pianetti, S., Kagan, H. M. and Sonenshein, G. E. (2003). Lysyl oxidase inhibits ras-mediated transformation by preventing activation of NF-kappa B. *Mol. Cell. Biol.* **23**, 2251-2263.

Kagan, H. M. and Li, W. (2003). Lysyl oxidase: properties, specificity, and biological roles inside and outside of the cell. *J. Cell. Biochem.* **88**, 660-672.

Kardon, G., Harfe, B. D. and Tabin, C. J. (2003). A Tcf4-positive mesodermal population provides a prepattern for vertebrate limb muscle patterning. *Dev. Cell* **5**, 937-944.

Kaufmann, M. H. (1992). *The Atlas of Mouse Development*. London: Elsevier Academic Press.

Li, H.-Y., Wang, Y., Heap, C. R., King, C.-H. R., Mundla, S. R., Voss, M., Clawson, D. K., Yan, L., Campbell, R. M., Anderson, B. D. et al. (2006). Dihydropyrrolopyrazole transforming growth factor-beta type I receptor kinase domain inhibitors: a novel benzimidazole series with selectivity versus transforming growth factor-beta type II receptor kinase and mixed lineage kinase-7. *J. Med. Chem.* **49**, 2138-2142.

Liu, D., Kang, J. S. and Derynck, R. (2004). TGF-beta-activated Smad3 represses MEF2-dependent transcription in myogenic differentiation. *EMBO J.* **23**, 1557-1566.

Lucero, H. A., Ravid, K., Grimsby, J. L., Rich, C. B., DiCamillo, S. J., Mäki, J. M., Myllyharju, J. and Kagan, H. M. (2008). Lysyl oxidase oxidizes cell membrane proteins and enhances the chemotactic response of vascular smooth muscle cells. *J. Biol. Chem.* **283**, 24103-24117.

Lucero, H. A., Mäki, J. M. and Kagan, H. M. (2011). Activation of cellular chemotactic responses to chemokines coupled with oxidation of plasma membrane proteins by lysyl oxidase. *J. Neural. Transm.* **118**, 1091-1099.

Luo, J., Tang, M., Huang, J., He, B.-C., Gao, J.-L., Chen, L., Zuo, G.-W., Zhang, W., Luo, Q., Shi, Q. et al. (2010). TGFbeta/BMP type I receptors ALK1 and ALK2 are essential for BMP9-induced osteogenic signaling in mesenchymal stem cells. *J. Biol. Chem.* **285**, 29588-29598.

Maeda, T., Sakabe, T., Sunaga, A., Sakai, K., Rivera, A. L., Keene, D. R., Sasaki, T., Stavnezer, E., Iannotti, J., Schweitzer, R. et al. (2011). Conversion of mechanical force into TGF-beta-mediated biochemical signals. *Curr. Biol.* **21**, 933-941.

Mäki, J. M. (2009). Lysyl oxidases in mammalian development and certain pathological conditions. *Histol. Histopathol.* **24**, 651-660.

Mäki, J. M., Räsänen, J., Tikkanen, H., Sormunen, R., Mäkikallio, K., Kivirikko, K. I. and Soininen, R. (2002). Inactivation of the lysyl oxidase gene Lox leads to aortic aneurysms, cardiovascular dysfunction, and perinatal death in mice. *Circulation* **106**, 2503-2509.

Mäki, J. M., Sormunen, R., Lippo, S., Kaarteenaho-Wiik, R., Soininen, R. and Myllyharju, J. (2005). Lysyl oxidase is essential for normal development and function of the respiratory system and for the integrity of elastic and collagen fibers in various tissues. *Am. J. Pathol.* **167**, 927-936.

Mathew, S. J., Hansen, J. M., Merrell, A. J., Murphy, M. M., Lawson, J. A., Hutcheson, D. A., Hansen, M. S., Angus-Hill, M. and Kardon, G. (2011). Connective tissue fibroblasts and Tcf4 regulate myogenesis. *Development* **138**, 371-384.

McLennan, I. S. (1993). Localisation of transforming growth factor beta 1 in developing muscles: implications for connective tissue and fiber type pattern formation. *Dev. Dyn.* **197**, 281-290.

Murphy, M. and Kardon, G. (2011). Origin of vertebrate limb muscle: the role of progenitor and myoblast populations. *Curr. Top. Dev. Biol.* **96**, 1-32.

Murphy, M. M., Lawson, J. A., Mathew, S. J., Hutcheson, D. A. and Kardon, G. (2011). Satellite cells, connective tissue fibroblasts and their interactions are crucial for muscle regeneration. *Development* **138**, 3625-3637.

Myllyharju, J. and Kivirikko, K. I. (2004). Collagens, modifying enzymes and their mutations in humans, flies and worms. *Trends Genet.* **20**, 33-43.

Neptune, E. R., Frischmeyer, P. A., Arking, D. E., Myers, L., Bunton, T. E., Gayraud, B., Ramirez, F., Sakai, L. Y. and Dietz, H. C. (2003). Dysregulation of TGF-beta activation contributes to pathogenesis in Marfan syndrome. *Nat. Genet.* **33**, 407-411.

Pischon, N., Mäki, J. M., Weisshaupt, P., Heng, N., Palamakumbura, A. H., N'Guessan, P., Ding, A., Radlanski, R., Renz, H., Bronckers, T. A. L. J. J. et al. (2009). Lysyl oxidase (lox) gene deficiency affects osteoblastic phenotype. *Calcif. Tissue Int.* **85**, 119-126.

Reynaud, C., Baas, D., Gleyzal, C., Le Guellec, D. and Sommer, P. (2008). Morpholino knockdown of lysyl oxidase impairs zebrafish development, and reflects some aspects of copper metabolism disorders. *Matrix Biol.* **27**, 547-560.

Riddle, R. D., Johnson, R. L., Laufer, E. and Tabin, C. (1993). Sonic hedgehog mediates the polarizing activity of the ZPA. *Cell* **75**, 1401-1416.

Rifkin, D. B. (2005). Latent transforming growth factor-beta (TGF-beta) binding proteins: orchestrators of TGF-beta availability. *J. Biol. Chem.* **280**, 7409-7412.

Salazar, V. S., Zarkadis, N., Huang, L., Norris, J., Grimston, S. K., Mbalaviele, G. and Civitelli, R. (2013). Embryonic ablation of osteoblast Smad4 interrupts matrix synthesis in response to canonical Wnt signaling and causes an osteogenesis-imperfecta-like phenotype. *J. Cell Sci.* **126**, 4974-4984.

Sasse, J., von der Mark, H., Kühl, U., Dessau, W. and von der Mark, K. (1981). Origin of collagen types I, III, and V in cultures of avian skeletal muscle. *Dev. Biol.* **83**, 79-89.

Saxena, V. K., Sundaresan, N. R., Malik, F., Ahmed, K. A., Saxena, M., Kumar, S., Nandedkar, P. V. and Singh, R. V. (2007). Temporal expression of transforming growth factor-beta2 and myostatin mRNA during embryonic myogenesis in Indian broilers. *Res. Vet. Sci.* **82**, 50-53.

Schweitzer, R., Chyung, J. H., Murtaugh, L. C., Brent, A. E., Rosen, V., Olson, E. N., Lassar, A. and Tabin, C. J. (2001). Analysis of the tendon cell fate using Scleraxis, a specific marker for tendons and ligaments. *Development* **128**, 3855-3866.

Seki, T., Hong, K.-H. and Oh, S. P. (2006). Nonoverlapping expression patterns of ALK1 and ALK5 reveal distinct roles of each receptor in vascular development. *Lab. Invest.* **86**, 116-129.

Development (2015) 142, 983-993 doi:10.1242/dev.113449

Serrano, A. L., Mann, C. J., Vidal, B., Ardite, E., Perdiguero, E. and Muñoz-Cánoves, P. (2011). Cellular and molecular mechanisms regulating fibrosis in skeletal muscle repair and disease. *Curr. Top. Dev. Biol.* **96**, 167-201.

Shi, Y. and Massagué, J. (2003). Mechanisms of TGF-beta signaling from cell membrane to the nucleus. *Cell* **113**, 685-700.

Spurney, C. F., Knoblach, S., Pistilli, E. E., Nagaraju, K., Martin, G. R. and Hoffman, E. P. (2008). Dystrophin-deficient cardiomyopathy in mouse: expression of Nox4 and Lox are associated with fibrosis and altered functional parameters in the heart. *Neuromuscul. Disord.* **18**, 371-381.

Warburton, D. and Shi, W. (2005). Lo, and the niche is knit: lysyl oxidase activity and maintenance of lung, aorta, and skin integrity. *Am. J. Pathol.* **167**, 921-922.

Yaffe, D. and Saxel, O. (1977). Serial passaging and differentiation of myogenic cells isolated from dystrophic mouse muscle. *Nature* **270**, 725-727.

Supplementary Figures:

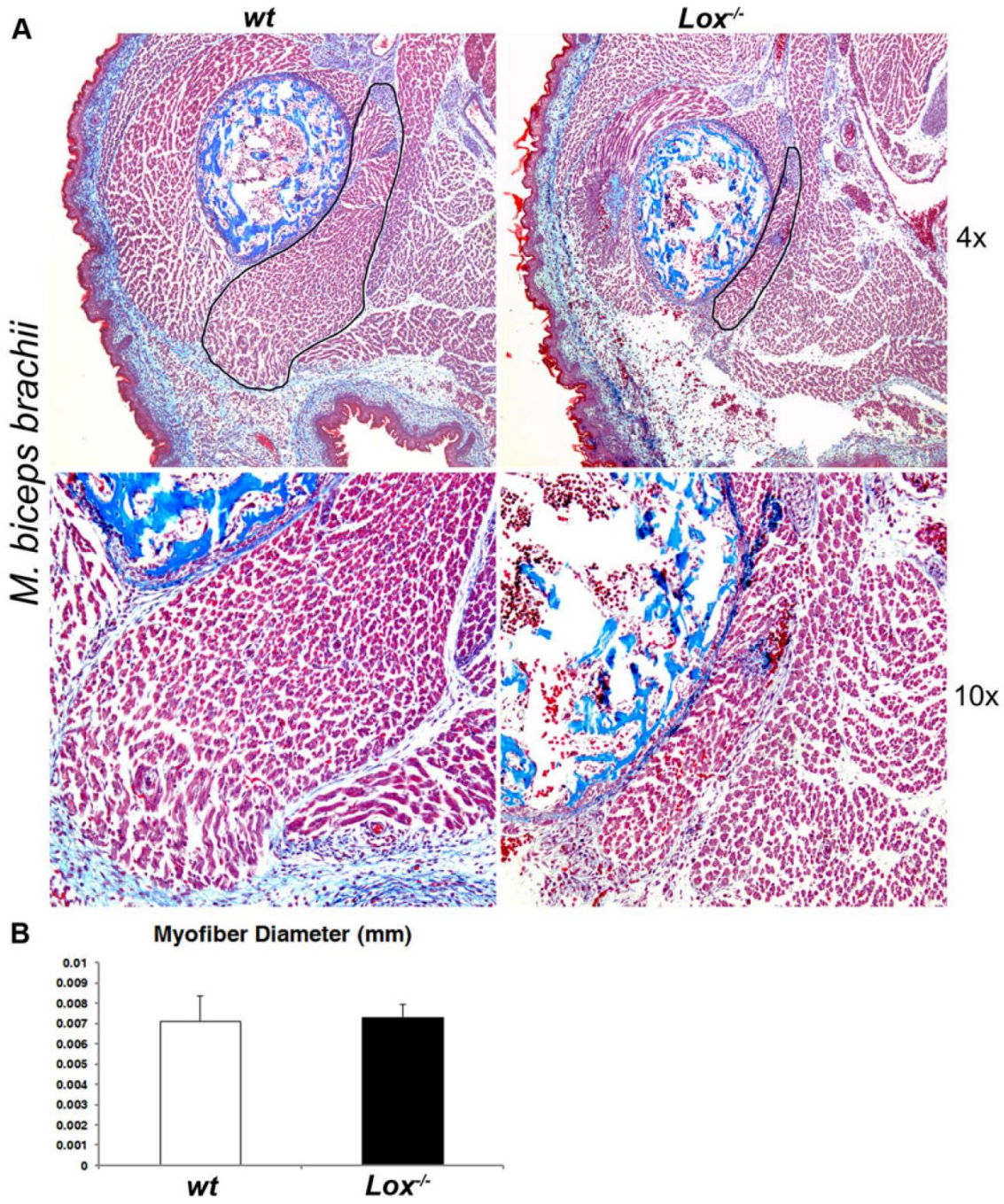

Figure S1: Muscles are smaller in *Lox*$^{-/-}$ mutants. Masson trichrome staining of M. Biceps brachii demonstrates smaller muscles and fewer myofibers in *Lox* mutants demonstrating phenotypes are not specific to zeugopod region (A). Myofiber diameter is not affected following *Lox* deletion (B).

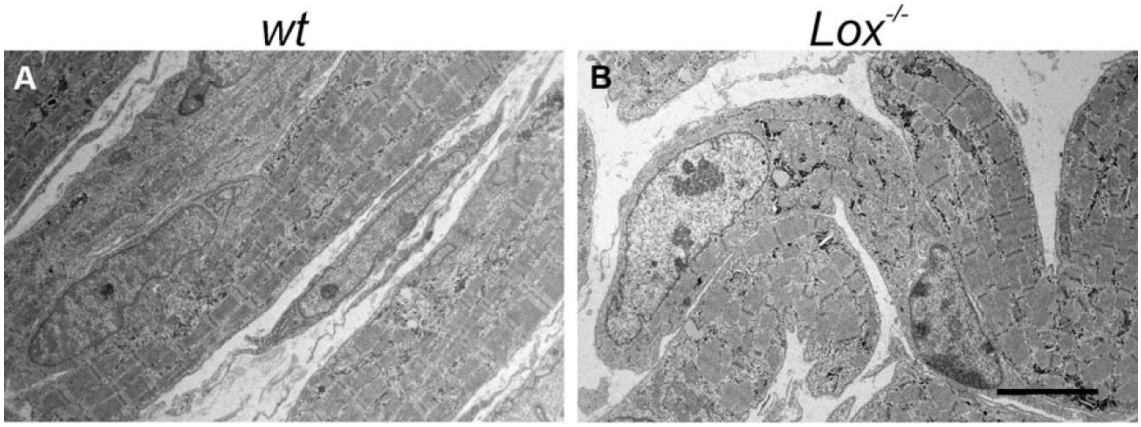

Figure S2: Ultrastructure of muscles is not lost in *Lox* mutants. TEM of images of muscles derived from E18.5 wild-type (*wt*; A) and *Lox* mutant (*Lox*$^{-/-}$; B) embryos. Although myofibers sometimes are curved in *Lox*$^{-/-}$ muscles, their overall sarcomeric organization is normal. Bar, 5 µm.

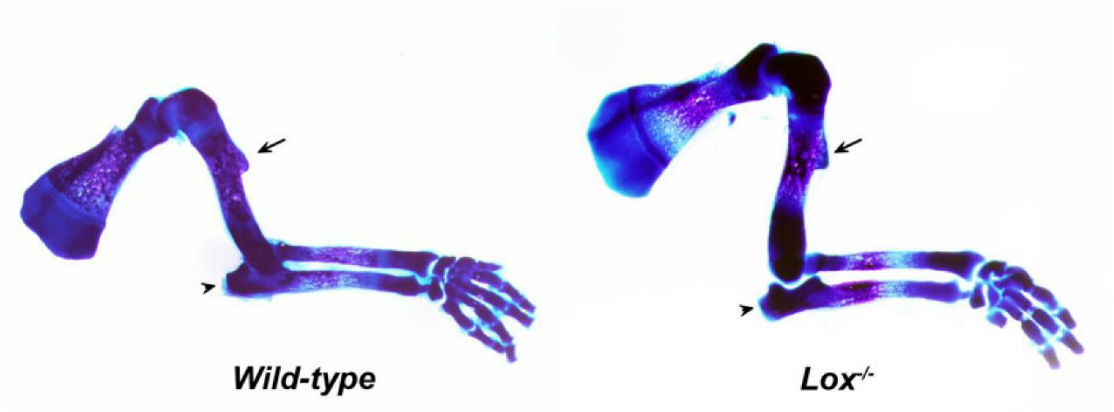

Figure S3: Lox does not regulate skeletal patterning. Skeletal preps of E18.5 forelimbs from *wt* (A) and *Lox*$^{-/-}$ (B) stained for alizarin red and alcian blue demonstrate the overall patterning of the skeleton is normal in Lox mutants. Note the olecranon processes (arrowheads) and deltoid tuberosities (arrows) are normally positioned and of comparable sizes in the two genotypes.

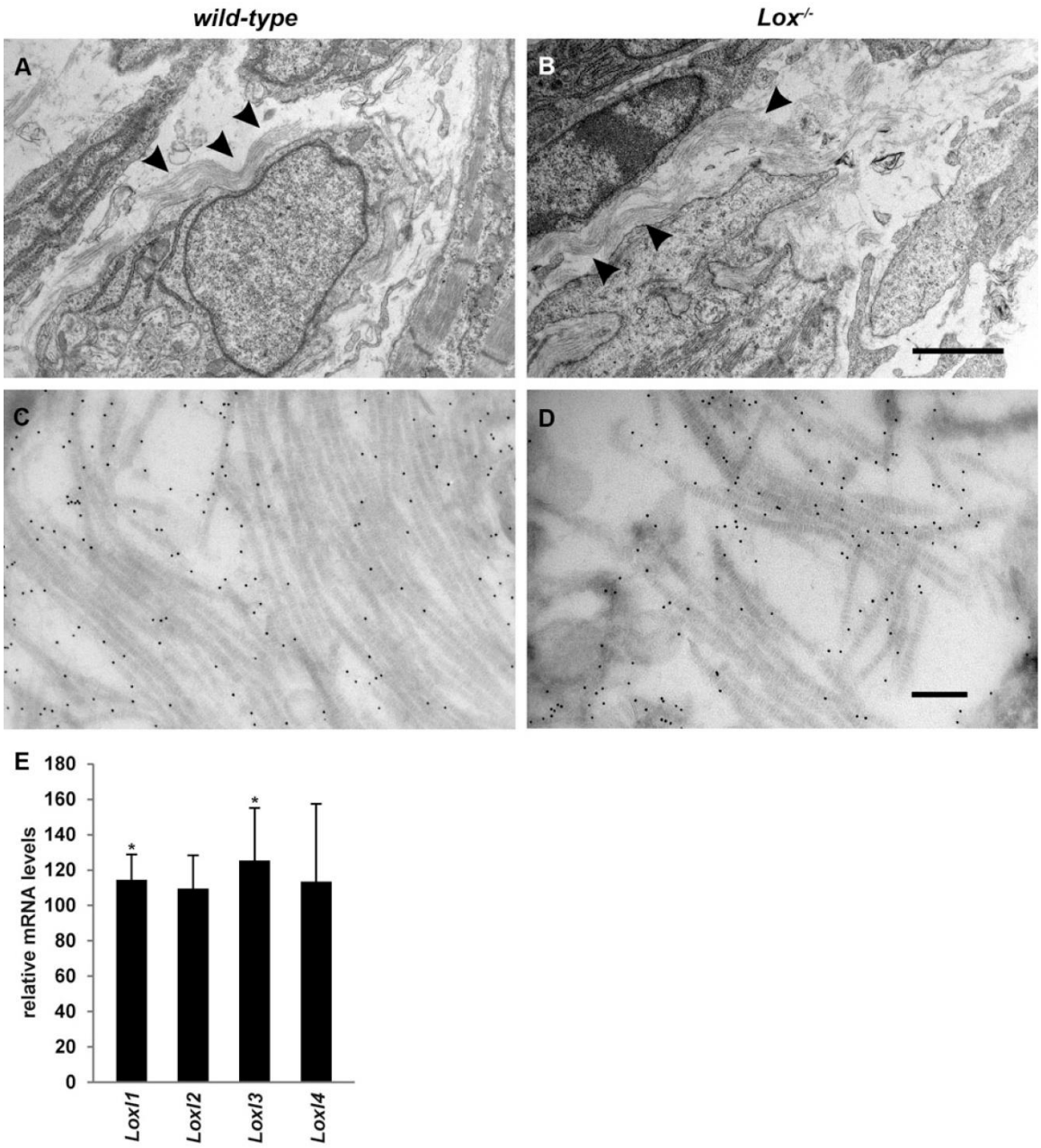

Figure S4: Collagen fibril organization is lost in *Lox*$^{-/-}$ muscles. TEM images derived from wild-type (A,C) and *Lox*$^{-/-}$ (B,D) of E18.5 embryos. Note that although collagen fibers are present in mutant muscles (black arrowheads, B) immuno-EM analysis using antibodies directed against ColI demonstrates collagen fibrils are disorganized in mutant muscles (C,D). Quantitative real time PCR analysis from muscle lysates for other members of the *Lox* family reveals *LoxL1* and *LoxL3* are significantly upregulated in mutants (E). Bars, 2 µm in A-B, and 200 nm in C-D.

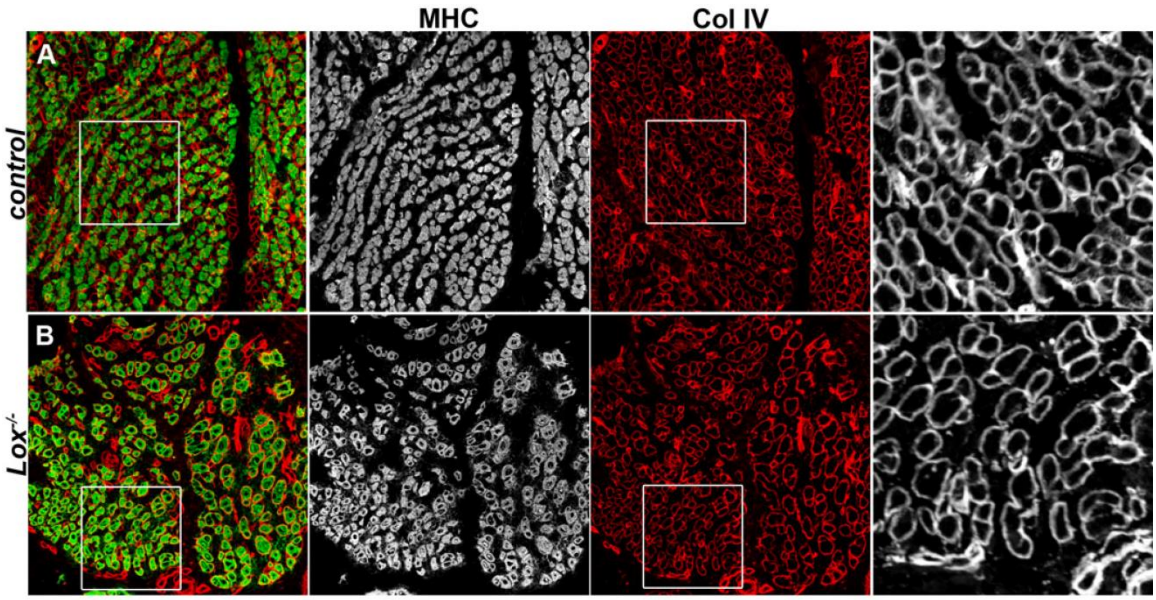

Figure S5: Collagen IV organization is not affected by Lox. Section immunostaining for Myosin (A4.1025; MHC) and for Collagen type IV (Col IV) on E18.5 muscle sections reveals that unlike ColI expression, that of Col IV is not disrupted in Lox mutant muscles (A,B).

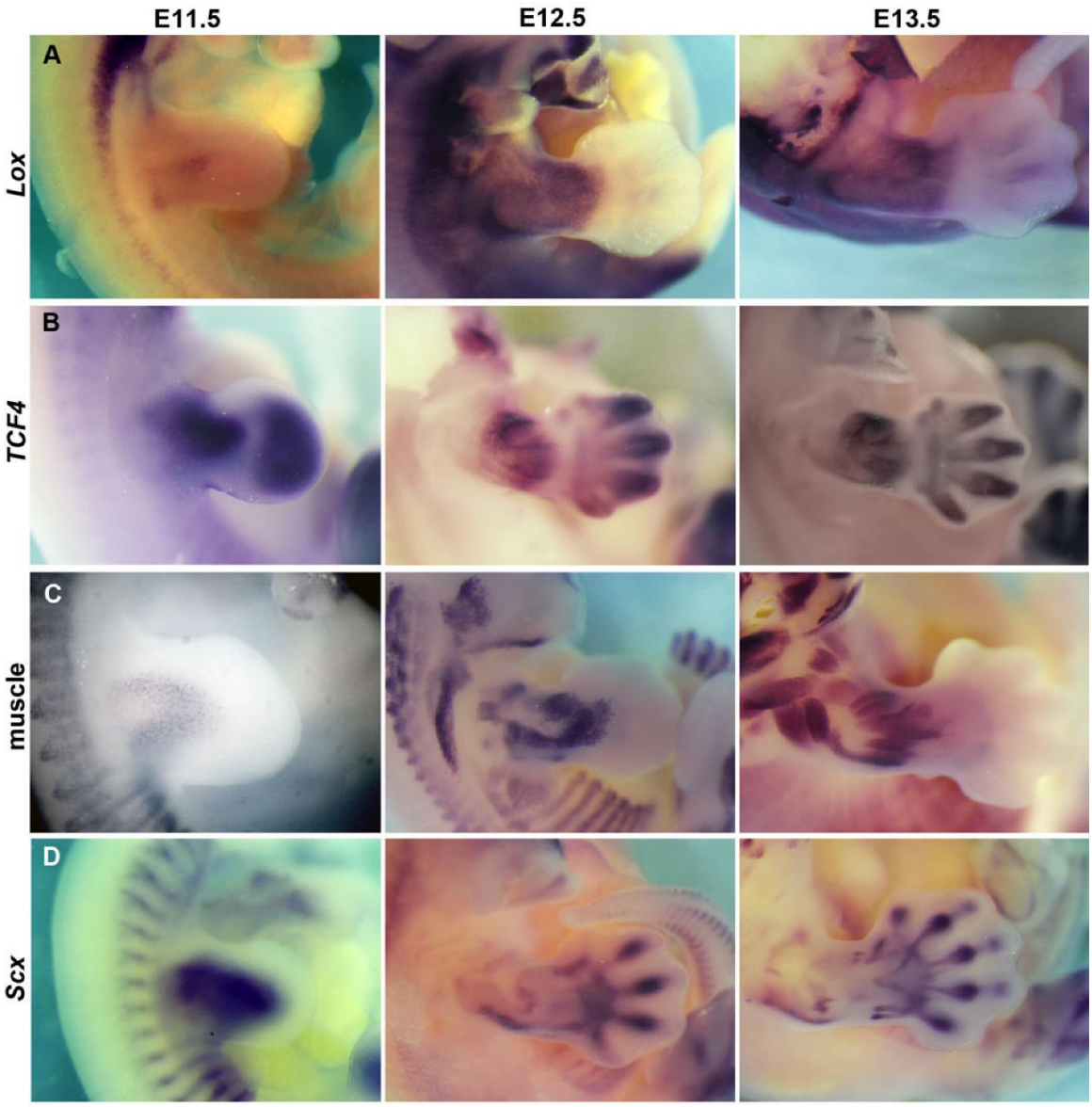

Figure S6: *Lox* expression in the developing limb. Whole-mount RNA *in situ* hybridization stainings for *Lox* (A), *Tcf4* marking the MCT fibroblasts (B), muscle progenitors marked by *Pax3* at E11.5 and *MyoD* at E12.5 and E13.5 (C) and *Scleraxis* (*Scx*) marking the tendon progenitors (D) at E11.5-E13.5. Note that *Lox* expression coincides with muscle development although its early expression is less well defined than that of *MyoD*.

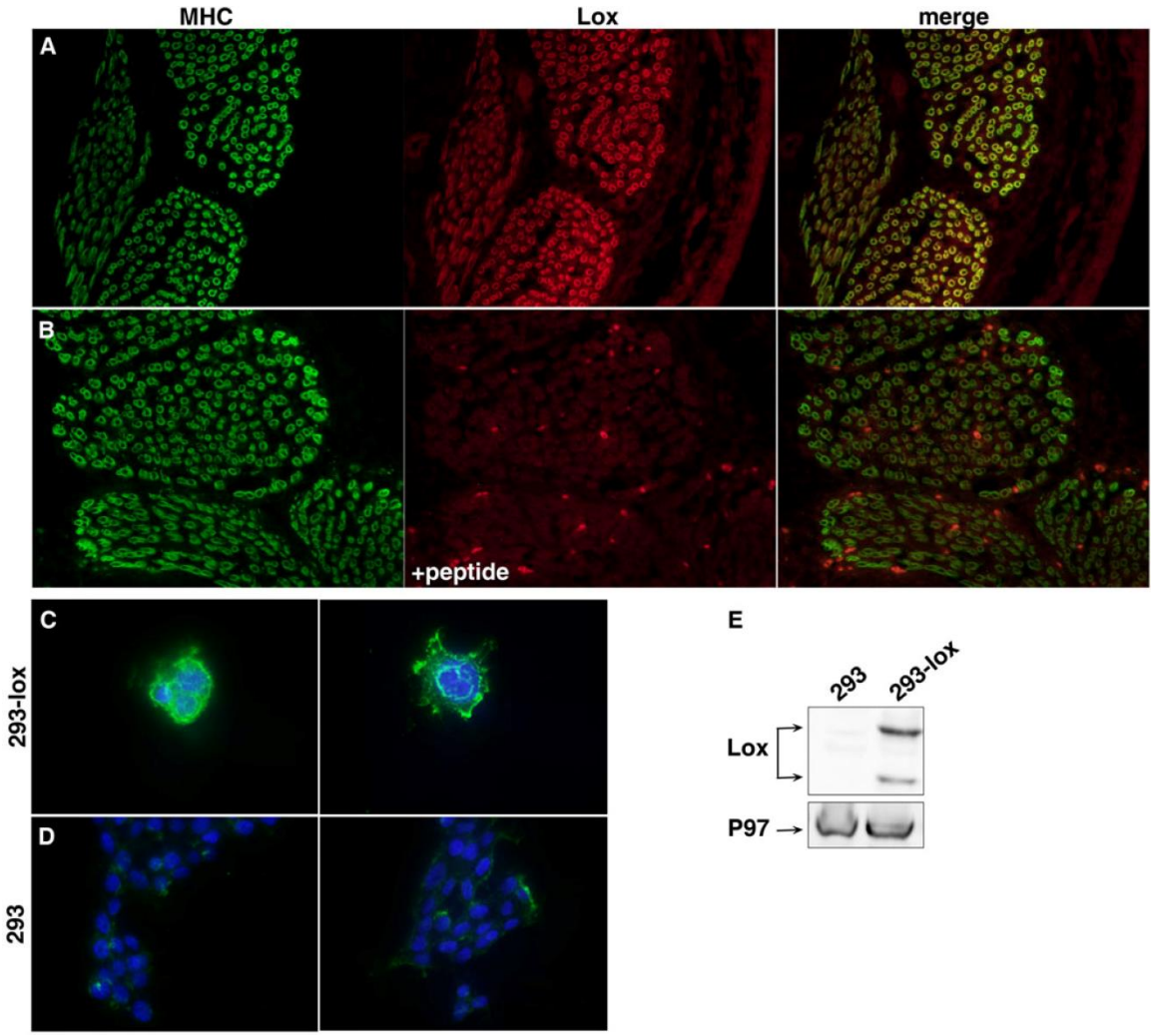

Figure S7: Lox antibody specificity. Lox antibody was raised against the EDTSCDYGYHRRFA peptide. Antibody specificity was tested using immunohistochemistry on paraffin sections (A,B), immunocytochemistry (C,D) and western blots (E). E15.5 sections were stained with anti-MHC (A4.1025, green) and anti-Lox (red) which was either pre-incubated with the peptide it was raised against or in blocking solution. Note that incubation with the peptide completely blocked staining suggesting the antibody specifically identifies this peptide (A,B). Mock or Lox transfected HEK 293 cells were stained for DAPI and Lox (green) (C,D) or lysed for a western blot analysis (E). Note the specific augmentation of Lox expression in cells over-expressing Lox.

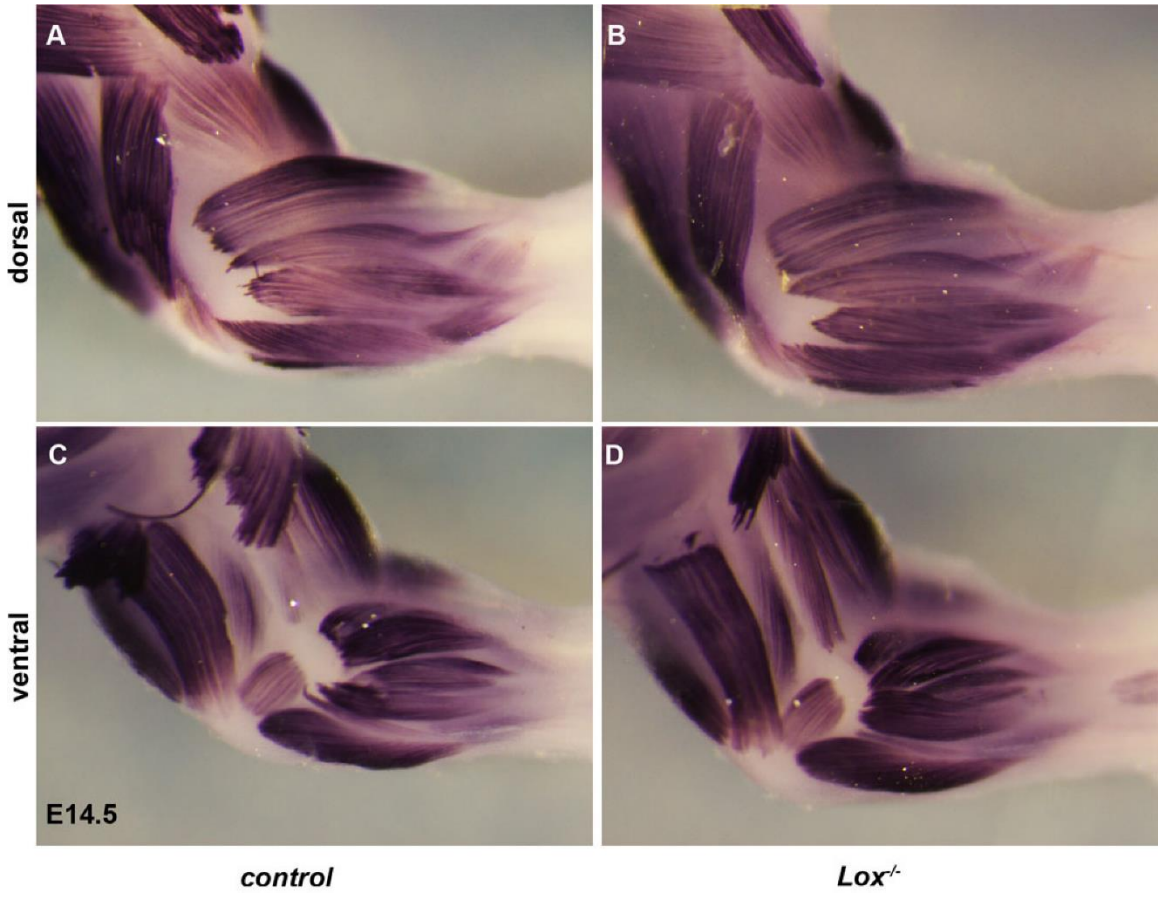

Figure S8: Muscle patterning defects and reduced myofiber amounts are not observed in *Lox* mutant limbs at E14.5. Whole-mount MHC (My32) of wild-type (A,C) and *Lox*$^{-/-}$ (B,D) demonstrates normal MHC expression at this stage.

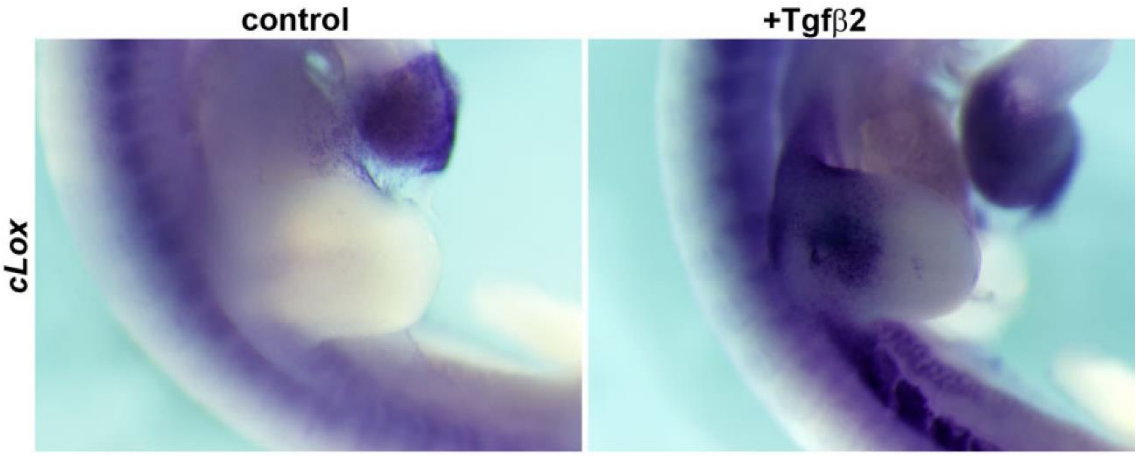

Figure S9: TGF-β regulates *Lox* expression. Beads soaked with PBS (control) implanted into chick limb bud do not induce *Lox* expression whereas those implanted with TGF-β2 (or TGF-β1) lead to strong ectopic *Lox* expression.

Supplemental materials and methods:

***In situ* hybridization:** Whole-mount RNA *in situ* hybridizations were carried out according to standard procedures, essentially as previously described (Riddle et al., 1993) on at least 3 mutant embryos at each stage. Most probes used were previously described: *MyoD* (Davis et al., 1987), *Scx* (Schweitzer et al., 2001), *Tcf4* (Kardon et al., 2003), *Myogenin* (Yee and Rigby, 1993). Mouse *Lox* probe was generated from an IMAGE clone (2655752, Source BioScience).

Immunohistochemistry: section immunohistochemistry was performed essentially as previously described (Hasson et al., 2010). The following antibodies were used: anti-Pax7 [1:10; Developmental Studies Hybridoma Bank (DHSB)]; anti-Laminin (1:200; Sigma); anti-Myosin (A4.1025, 1:10; DSHB]; anti-Myosin (My32; 1:800; Sigma); ColI (1:200; Abcam); ColIV (1:200; Abcam); anti-Tcf4 (1:200; Millipore); anti-Tcf4 (1:100; Cell Signaling); anti-pSMAD2 (3108; Cell Signaling; 1:100); several anti-Lox antibodies were used which gave similar results (1:200 from Abcam, Novus Biologicals, LSBio and generated by GenScript). Anti-My32 (1:800; Sigma) whole-mount immunohistochemistry was carried out essentially as described in (Hasson et al., 2010).

Isolation of mouse embryonic fibroblasts (MEFs): E14.5 embryos were decapitated and sliced into pieces. Pieces were incubated with trypsin for 15 min. Tissues were pipetted through and more trypsin were added and incubation was continued for 5 min. Cell and tissue mix was first washed with Dulbecco's modified Eagle's medium (Invitrogen Corp.) containing 20% fetal bovine serum (v/v), 5 mM L-glutamine, 1% nonessential amino acids, 2x penicillin and streptomycin (PS), 250 µg/ml amphotericin B and then plated in the same medium. Cultures of fibroblast that formed around tissue pieces were trypsinized, passaged, expanded and genotyped. 2x PS was used within first two cell divisions and 20% FBS was gradually decreased to 10%. MEFs were used up to a maximum of 9 passages.

Phosphorylated SMAD Western blot: MEFs were grown in medium described above. Cells were incubated with different concentration of mouse recombinant TGF-β1 (7666-MB-005, R&B Systems) for different periods of time and then lysed with a buffer (50 mM HEPES, 150 mM NaCl, 1 mM EDTA, 10 % glycerol, 0.1 % Tween 20, 1 % NP-40, 2.5 mM EGTA) on ice for 20 min. The supernatant protein concentrations were determined using the Bradford technique (Bio-Rad protein assay). Supernatants were resolved by SDS-PAGE and blotted onto Immobilon-P membranes (Millipore). Western blots were blocked with Tris-bufferd saline with 5% nonfat dry milk and probed with the following primary antibodies: Phospo-Smad2 (3108; Cell Signaling), Smad2 (5339; Cell Signaling) and anti-α-tubulin (B-6199;

Sigma-Aldrich). Bound antibodies were detected with horseradish peroxidase-conjugated secondary antibodies (Dako) and ECL detection reagents (Thermo Scientific and Millipore).

Luciferase Analysis: The TGF-β pathway analysis was performed using Cignal SMAD Reporter Assay Kit (CCS-017L; Qiagen). Briefly, 30 000 cells were plated into 12-well plates and next day cells were transfected with pathway reporters using FuGENE HD transfection reagent (Promega) according to manufacturer's protocol. Recombinant TGF-β was added to samples for the designated time. Cells were lysed on the following day and luciferase measured with Dual-Luciferase Reporter Assay System (Promega).

Collagen measurements: The amount of collagen within *wt* and *Lox*$^{-/-}$ E18.5 forelimb muscles was measured using the hydroxyproline assay while following the user's manual (Chondrex). Briefly, subsequent to tissue hydrolysis in 10N HCl at 120C for 24 hours hydroxyproline levels were measured. Based on that, collagen levels which contain 13.5% hydroxyproline, were calculated.

TGF-β activation: Affi-gel beads (153-7301; Bio-Rad) were washed in PBS and incubated for 1 hr with TGF-β1 and TGF-β2 (R&D Systems) on ice. Beads were then implanted *in ovo* in lateral plate mesoderm and early limb bud of HH St. 18-19 and embryos were harvested 24-48 hrs later.

Lox knockdown using shRNA: HEK293-T cells were co-transfected with 8µg of the Lox MISSION shRNA lentiviral plasmid (SHCLNG-NM_010728) or with a shRNA control plasmid (SHC003), with lenti packaging PAX2 vector and with VSVG envelope vector using Lipofectamine-2000 reagent according to the vendor's instructions. The cells were then incubated in 37°C for 16-24 hours. The conditioned medium containing viruses, was collected and filtered through 0.45µm filters. C2C12 cells were incubated with the virus-containing medium in the presence of Polybrene (Sigma H9268, 8µg/ml) for 16 hours. After the first incubation, cells were washed twice with PBS and incubated with fresh growth medium with puromycin (2µg/ml).

Histology of skeletal elements:

Newborn pups were skinned and eviscerated and then stained for 24-48 hours in 0.06% Alizarin red S and 0.014% Alcian blue (final concentrations). Skeletons were then cleared in KOH followed by glycerol for imaging.

Table S1: qRT-PCR oligos

Binding site in template	Primer sequences (5' to 3')	Product size (bp)
Tgfβ1, forward Tgfβ1, reserve	GAGCCCGAAGCGGACTACTA TGGTTTTCTCATAGATGGCGTTG	82
Tgfβ2, forward Tgfβ2, reserve	AGTTTACACTGCCCCTGCTG AGAGGTGCCATCAATACCTGC	105
Tgfβ3, forward Tgfβ3, reserve	CACCACAACCCACACCTGAT CAGGTTGCGGAAGCAGTAAT	117
Ctgf, forward Ctgf, reserve	GGGCCTCTTCTGCGATTTC ATCCAGGCAAGTGCATTGGTA	151
α-Sma, forward α-Sma, reserve	GTCCCAGACATCAGGGAGTAA TCGGATACTTCAGCGTCAGGA	102
Col1a2, forward Col1a2, reserve	AAGGGTGCTACTGGACTCCC TTGTTACCGGATTCTCCTTTGG	155
Col3a1, forward Col3a1, reserve	CTGTAACATGGAAACTGGGGAAA CCATAGCTGAACTGAAAACCACC	144

Table S2: TGFβ inhibition rescues *Lox*$^{-/-}$ muscle patterning defects

* EDC and ECR in mutants were considered as the muscles at the location of their normal counterparts.

	Wild-type	***Lox*$^{-/-}$**	***Lox*$^{-/-}$ + TGFβ inhibitor**
EDC* length	100±10.4 (n=6)	76.6±33.4 (n=6)	92.7±15.7 (n=8)
ECR* length	100±9.5 (n=6)	79.8±34 (n=6)	85.6±27.7 (n=8)

Supplementary References:

Davis, R. L., Weintraub, H. and Lassar, A. B. (1987). Expression of a single transfected cDNA converts fibroblasts to myoblasts. *Cell* **51**, 987-1000.

Hasson, P., DeLaurier, A., Bennett, M., Grigorieva, E., Naiche, L. A., Papaioannou, V. E., Mohun, T. J. and Logan, M. P. (2010). Tbx4 and Tbx5 acting in connective tissue are required for limb muscle and tendon patterning. *Developmental cell* **18**, 148-156.

Kardon, G., Harfe, B. D. and Tabin, C. J. (2003). A Tcf4-positive mesodermal population provides a prepattern for vertebrate limb muscle patterning. *Developmental cell* **5**, 937-944.

Riddle, R. D., Johnson, R. L., Laufer, E. and Tabin, C. (1993). Sonic hedgehog mediates the polarizing activity of the ZPA. *Cell* **75**, 1401-1416.

Schweitzer, R., Chyung, J. H., Murtaugh, L. C., Brent, A. E., Rosen, V., Olson, E. N., Lassar, A. and Tabin, C. J. (2001). Analysis of the tendon cell fate using Scleraxis, a specific marker for tendons and ligaments. *Development (Cambridge, England)* **128**, 3855-3866.

Yee, S. P. and Rigby, P. W. (1993). The regulation of myogenin gene expression during the embryonic development of the mouse. *Genes Dev* **7**, 1277-1289.